

Models for extremal dependence derived from skew-symmetric families

B. Beranger, S. A. Padoan and S. A. Sisson

Abstract

Skew-symmetric families of distributions such as the skew-normal and skew- t represent supersets of the normal and t distributions, and they exhibit richer classes of extremal behaviour. By defining a non-stationary skew-normal process, which allows the easy handling of positive definite, non-stationary covariance functions, we derive a new family of max-stable processes – the extremal-skew- t process. This process is a superset of non-stationary processes that include the stationary extremal- t processes. We provide the spectral representation and the resulting angular densities of the extremal-skew- t process, and illustrate its practical implementation

Keywords: Asymptotic independence; Angular density; Extremal coefficient; Extreme values; Max-stable distribution; Non-central extended skew- t distribution; Non-stationarity; Skew-Normal distribution; Skew-Normal process; Skew- t distribution.

1 Introduction

The modern-day analysis of extremes is based on results from the theory of stochastic processes. In particular, max-stable processes (de Haan, 1984) are a popular and useful tool when modelling extremal responses in environmental, financial and engineering applications. Let $\mathbb{S} \subseteq \mathbb{R}^k$ denote a k -dimensional region of space (or space-time) over which a real-valued stochastic process $\{Y(s)\}_{s \in \mathbb{S}}$ with a continuous sample path on \mathbb{S} can be defined. Considering a sequence Y_1, \dots, Y_n of *iid* copies of Y , the pointwise partial maximum can be defined as

$$M_n(s) = \max_{i=1, \dots, n} Y_i(s), \quad s \in \mathbb{S}.$$

If there are sequences of real-valued functions, $a_n(s) > 0$ and $b_n(s)$, for $s \in \mathbb{S}$ and $n = 1, 2, \dots$, such that

$$\left\{ \frac{M_n(s) - b_n(s)}{a_n(s)} \right\}_{s \in \mathbb{S}} \Rightarrow \{U(s)\}_{s \in \mathbb{S}},$$

converges weakly as $n \rightarrow \infty$ to a process $U(s)$ with non-degenerate marginal distributions for all $s \in \mathbb{S}$, then $U(s)$ is known as a max-stable process (de Haan and Ferreira, 2006, Ch. 9). In this setting, for a finite sequence of points $(s_j)_{j \in I}$ in some index set $I = \{1, \dots, d\}$, the finite-dimensional distribution of U is then a multivariate extreme value distribution (de Haan and Ferreira, 2006, Ch. 6). This distribution has generalised extreme value univariate margins and, when parameterised with unit Fréchet margins, has a joint distribution function of the form

$$G(x_j, j \in I) = \exp\{-V(x_j, j \in I)\}, \quad x_j > 0,$$

where $x_j \equiv x(s_j)$. The exponent function V describes the dependence between extremes, and can be expressed as

$$V(x_j, j \in I) = \int_{\mathbb{W}} \max_{j \in I} (w_j/x_j) H(dw_1, \dots, dw_d),$$

where the angular measure H is a finite measure defined on the d -dimensional unit simplex $\mathbb{W} = \{w \in \mathbb{R}^d : w_1 + \dots + w_d = 1\}$, satisfying the moment conditions $\int_{\mathbb{W}} w_j H(dw) = 1, j \in I$, (de Haan and Ferreira, 2006, Ch. 6).

In recent years a variety of specific max-stable processes have been developed, many of which have become popular as they can be practically amenable to statistical modelling (Davison et al., 2012). The extremal- t process (Opitz, 2013) is one of the best-known and widely-used max-stable processes. It contains the Brown-Resnick process (Brown and Resnick, 1977, Kabluchko et al., 2009), the Gaussian extreme-value process (Smith, 1990) and the extremal-Gaussian processes (Schlather, 2002) as special cases. In their most basic form, the Brown-Resnick and the extremal- t processes can be respectively understood as the limiting extremal processes of strictly stationary Gaussian and Student- t processes. However, in practice, data may be non-stationary and exhibit asymmetric distributions in many applications. In these scenarios, skew-symmetric distributions (Azzalini, 2013, Arellano-Valle and Azzalini, 2006, Azzalini, 2005, Genton, 2004, Azzalini, 1985) provide simple models for modelling asymmetrically distributed data. However, the limiting extremal behaviour of these processes has not yet been established.

In this paper we characterise and develop statistical models for the extremal behaviour of skew-normal and skew- t distributions. The joint tail behaviours of these skew distributions are capable of describing a far wider range of dependence levels than that obtained under the symmetric normal and t distributions. We provide a definition of a skew-normal process which is in turn a non-stationary process. This provides an accessible approach to constructing positive definite, non-stationary covariance functions when working with non-Gaussian processes. Recently some forms of non-stationary dependent structures embedded into max-stable processes have been studied by Huser and Genton (2015). We show that on the basis of the skew-normal process a new family of max-stable processes – the extremal-skew- t process – can be obtained. This process is a superset of non-stationary processes that includes the stationary extremal- t processes (Opitz, 2013). From the extremal-skew- t process, a rich family of non-stationary, isotropic or anisotropic extremal coefficient functions can be obtained.

This paper is organised as follows: in Section 2 we first introduce a new variant of the extended skew- t class of distributions, before developing a non-stationary version of the skew-normal process. In Section 3 we derive some asymptotic results for the skew-normal and t distributions, provide the spectral representation of the extended extremal skew- t process, and derive the angular density of the extremal skew- t distribution. Section 4 discusses inferential aspects, and presents a simulated analysis. We conclude with a Discussion.

2 Preliminary results on skew-normal processes and skew- t distributions

We first present two preliminary results that will be used for our main contribution in Section 3. Hereafter, we use $Y \sim \mathcal{D}_d(\theta_1, \theta_2, \dots)$ to denote that Y is a d -dimensional random vector with probability law \mathcal{D} and parameters $\theta_1, \theta_2, \dots$. When $d = 1$ the subscript is omitted for brevity. Similarly, when a parameter is equal to zero or a scale matrix is equal to the identity (both in a vector and scalar sense) so that \mathcal{D}_d reduces to an obvious sub-family, it is also omitted.

2.1 The non-central, extended skew- t distribution

While several skew-symmetric distributions have been developed (see e.g. Genton (2004) and Azzalini (2013)), we focus on the skew-normal and skew- t distributions. In order to present our main results, we first introduce a new variant of the extended skew- t class (Arellano-Valle and

Genton, 2010), namely the *non-central*, extended skew-*t* family of distributions.

Denote a d -dimensional skew-normally distributed random vector by $Y \sim \mathcal{SN}_d(\mu, \Omega, \alpha, \tau)$ (Arellano-Valle and Genton, 2010). This random vector has probability density function (pdf)

$$\phi_d(y; \mu, \Omega, \alpha, \tau) = \frac{\phi_d(y; \mu, \Omega)}{\Phi\{\tau/\sqrt{1 + Q_{\bar{\Omega}}(\alpha)}\}} \Phi(\alpha^\top z + \tau), \quad y \in \mathbb{R}^d, \quad (1)$$

where $\phi_d(y; \mu, \Omega)$ is a d -dimensional normal pdf with mean $\mu \in \mathbb{R}^d$ and $d \times d$ covariance matrix Ω , $z = (y - \mu)/\omega$, $\omega = \text{diag}(\Omega)^{1/2}$, $\bar{\Omega} = \omega^{-1} \Omega \omega^{-1}$, $Q_{\bar{\Omega}}(\alpha) = \alpha^\top \bar{\Omega} \alpha$ and $\Phi(\cdot)$ is the standard univariate normal cdf. The shape parameters $\alpha \in \mathbb{R}^d$ and $\tau \in \mathbb{R}$ are respectively *slant* and *extension* parameters. The cdf associated with (1) is termed the extended skew-normal distribution (Arellano-Valle and Genton, 2010) of which the skew-normal and normal distributions are special cases (Arellano-Valle and Genton, 2010, Azzalini, 2013). For example, in the case where $\alpha = 0$ and $\tau = 0$ the standard normal pdf is recovered.

A generalisation of (1) is the extended skew-*t* family, introduced by Arellano-Valle and Genton (2010). We further generalise this family, as follows:

Definition 1. Y is a d -dimensional, non-central extended skew-*t* distributed random vector, denoted by $Y \sim \mathcal{ST}_d(\mu, \Omega, \alpha, \tau, \kappa, \nu)$, if for $y \in \mathbb{R}^d$ it has pdf

$$\psi_d(y; \mu, \Omega, \alpha, \tau, \kappa, \nu) = \frac{\psi_d(y; \mu, \Omega, \nu)}{\Psi\left(\frac{\tau}{\sqrt{1+Q_{\bar{\Omega}}(\alpha)}}; \frac{\kappa}{\sqrt{1+Q_{\bar{\Omega}}(\alpha)}}, \nu\right)} \Psi\left\{(\alpha^\top z + \tau)\sqrt{\frac{\nu + d}{\nu + Q_{\bar{\Omega}^{-1}}(z)}}; \kappa, \nu + d\right\}, \quad (2)$$

where $\psi_d(y; \mu, \Omega, \nu)$ is the pdf of a d -dimensional *t*-distribution with location $\mu \in \mathbb{R}^d$, $d \times d$ scale matrix Ω and $\nu \in \mathbb{R}^+$ degrees of freedom, $\Psi(\cdot; a, \nu)$ denotes a univariate non-central *t* cdf with non-centrality parameter $a \in \mathbb{R}$ and ν degrees of freedom, and $Q_{\bar{\Omega}^{-1}}(z) = z^\top \bar{\Omega}^{-1} z$. The remaining terms are as defined in (1). The associated cdf is

$$\Psi_d(y; \mu, \Omega, \alpha, \tau, \kappa, \nu) = \frac{\Psi_{d+1}\{\bar{z}; \Omega^*, \kappa^*, \nu\}}{\Psi(\bar{\tau}; \bar{\kappa}, \nu)}, \quad (3)$$

where $\bar{z} = (z^\top, \bar{\tau})^\top$, Ψ_{d+1} is a $(d+1)$ -dimensional (non-central) *t* cdf with covariance matrix and non-centrality parameters

$$\Omega^* = \begin{pmatrix} \bar{\Omega} & -\delta \\ -\delta^\top & 1 \end{pmatrix}, \quad \kappa^* = \begin{pmatrix} 0 \\ \bar{\kappa} \end{pmatrix},$$

and ν degrees of freedom, and where

$$\delta = \{1 + Q_{\bar{\Omega}}(\alpha)\}^{-1/2} \bar{\Omega} \alpha, \quad \bar{\kappa} = \{1 + Q_{\bar{\Omega}}(\alpha)\}^{-1/2} \kappa, \quad \bar{\tau} = \{1 + Q_{\bar{\Omega}}(\alpha)\}^{-1/2} \tau. \quad (4)$$

This definition includes the extended skew-*t* family of Arellano-Valle and Genton (2010) as a special case when the non-centrality parameter κ is zero. When Y is skew-*t* distributed according to Definition 1, similar properties to those discussed in Arellano-Valle and Genton (2010) can be derived.

Proposition 1 (Properties). *Let $Y \sim \mathcal{ST}_d(\mu, \Omega, \alpha, \tau, \kappa, \nu)$.*

1. *Marginal and conditional distributions.* *Let $I \subset \{1, \dots, d\}$ and $\bar{I} = \{1, \dots, d\} \setminus I$ identify the d_I - and $d_{\bar{I}}$ -dimensional subvector partition of Y such that $Y = (Y_I^\top, Y_{\bar{I}}^\top)^\top$, with corresponding partitions of the parameters (μ, Ω, α) . Then*

(a) $Y_I \sim \mathcal{ST}_{d_I}(\mu_I, \Omega_{II}, \alpha_I^*, \tau_I^*, \kappa_I^*, \nu)$, where

$$\alpha_I^* = \frac{\alpha_I + \bar{\Omega}_{II}^{-1} \bar{\Omega}_{I\bar{I}} \alpha_{\bar{I}}}{\sqrt{1+Q_{\bar{\Omega}_{II\cdot I}}(\alpha_I)}}, \quad \tau_I^* = \frac{\tau}{\sqrt{1+Q_{\bar{\Omega}_{II\cdot I}}(\alpha_I)}}, \quad \kappa_I^* = \frac{\kappa}{\sqrt{1+Q_{\bar{\Omega}_{II\cdot I}}(\alpha_I)}}, \quad (5)$$

given $\tilde{\Omega}_{\bar{I}\bar{I}\cdot I} = \bar{\Omega}_{\bar{I}\bar{I}} - \bar{\Omega}_{\bar{I}I} \bar{\Omega}_{II}^{-1} \bar{\Omega}_{I\bar{I}}$.

(b) $(Y_{\bar{I}}|Y_I = y_I) \sim \mathcal{ST}_{d_{\bar{I}}}(\mu_{\bar{I}\cdot I}, \Omega_{\bar{I}\cdot I}, \alpha_{\bar{I}\cdot I}, \tau_{\bar{I}\cdot I}, \kappa_{\bar{I}\cdot I}, \nu_{\bar{I}\cdot I})$, where $\mu_{\bar{I}\cdot I} = \mu_{\bar{I}} + \Omega_{I\bar{I}} \Omega_{II}^{-1} (y_I - \mu_I)$, $\Omega_{\bar{I}\cdot I} = \zeta_I \Omega_{\bar{I}\bar{I}\cdot I}$, $\zeta_I = \{\nu + Q_{\Omega_{II}^{-1}}(z_I)\}/(\nu + d_I)$, $z_I = \omega_I^{-1}(y_I - \mu_I)$, $\omega_I = \text{diag}(\omega_{II})^{1/2}$, $Q_{\Omega_{II}^{-1}}(z_I) = z_I^\top \Omega_{II}^{-1} z_I$, $\Omega_{\bar{I}\bar{I}\cdot I} = \bar{\Omega}_{\bar{I}\bar{I}} - \bar{\Omega}_{\bar{I}I} \bar{\Omega}_{II}^{-1} \bar{\Omega}_{I\bar{I}}$, $\alpha_{\bar{I}\cdot I} = \omega_{\bar{I}\cdot I} \omega_{\bar{I}}^{-1} \alpha_{\bar{I}}$, $\omega_{\bar{I}\cdot I} = \text{diag}(\Omega_{\bar{I}\bar{I}\cdot I})^{1/2}$, $\omega_{\bar{I}} = \text{diag}(\omega_{\bar{I}\bar{I}})^{1/2}$, $\tau_{\bar{I}\cdot I} = \zeta_I^{-1/2} \{(\alpha_{\bar{I}}^\top \bar{\Omega}_{\bar{I}\bar{I}} \bar{\Omega}_{II}^{-1} + \alpha_I^\top) z_I + \tau\}$, $\kappa_{\bar{I}\cdot I} = \zeta_I^{-1/2} \kappa$ and $\nu_{\bar{I}\cdot I} = \nu + d_I$.

2. *Conditioning type stochastic representation.* We can write $Y = \mu + \Omega Z$, where $Z = (X|\alpha^\top X + \tau > X_0)$, and where $X \sim \mathcal{T}_d(\bar{\Omega}, \nu)$ is independent of $X_0 \sim \mathcal{T}(\kappa, \nu)$.

3. *Additive type stochastic representation.* We can write $Y = \mu + \Omega Z$, where $Z = \sqrt{\frac{\nu + \tilde{X}_0^2}{\nu + 1}} X_1 + \delta \tilde{X}_0$, $X_1 \sim \mathcal{T}_d(\Omega - \delta \tau^\top, \bar{\kappa}, \nu + 1)$ is independent of $\tilde{X}_0 = (X_0|X_0 + \bar{\tau} > 0)$, $X_0 \sim \mathcal{T}(\bar{\kappa}, \nu)$, $\delta \in (-1, 1)^d$ and where $\bar{\tau}$ and $\bar{\kappa}$ are as in (4).

Proof in Appendix A.1

We now present our second preliminary result – the development of a new non-stationary, skew normal random process.

2.2 A non-stationary, skew-normal random process

While there are several definitions of a stationary skew-normal process (e.g. Minozzo and Feracuti, 2012), stationarity is incompatible with the requirement that all finite-dimensional distributions of the process are skew-normal. We now construct a non-stationary version of the skew-normal process through the additive-type stochastic representation (e.g. Azzalini, 2013, Ch. 5). A similar approach was explored by Zhang and El-Shaarawi (2010) for the stationary case.

Definition 2. Let $\{X(s)\}_{s \in \mathbb{S}}$ be a stationary Gaussian random process on \mathbb{S} with zero mean, unit variance and correlation function $\rho(h) = \mathbb{E}\{X(s)X(s+h)\}$ for $s \in \mathbb{S}$ and $h \in \mathbb{R}^k$. For $X' \sim \mathcal{N}(0, 1)$ independent of $X(s)$, $\varepsilon \in \mathbb{R}$ and a function $\delta : \mathbb{S} \mapsto (-1, 1)$, define

$$\begin{aligned} X''(s) &:= X'|X' + \varepsilon > 0, & \forall s \in \mathbb{S} \\ Z(s) &:= \sqrt{1 - \delta(s)^2} X(s) + \delta(s) X''(s), & s \in \mathbb{S}. \end{aligned} \quad (6)$$

Then $Z(s)$ is a skew-normal random process.

We refer to $\delta(s)$ as the slant function. From (6), if $\delta(s) \equiv 0$ for all $s \in \mathbb{S}$, then Z is a Gaussian random process. Note that Z is a random process with a consistent family of distribution functions, since $Z(s) = a(s)X(s) + b(s)Y(s)$ where a and b are bounded functions and X and Y are random processes with a consistent family of distribution functions. For any finite sequence of points $s_1, \dots, s_d \in \mathbb{S}$ the joint distribution of $Z(s_1), \dots, Z(s_d)$ is $\mathcal{SN}_d(\bar{\Omega}, \alpha, \tau)$, where

$$\begin{aligned} \bar{\Omega} &= D_\delta(\bar{\Sigma} + (D_\delta^{-1} \delta)(D_\delta^{-1} \delta)^\top) D_\delta \\ \alpha &= \{1 + (D_\delta^{-1} \delta)^\top \bar{\Sigma}^{-1} (D_\delta^{-1} \delta)\}^{-1/2} D_\delta^{-1} \bar{\Sigma}^{-1} (D_\delta^{-1} \delta) \\ \tau &= \{1 + Q_{\bar{\Omega}}(\alpha)\}^{1/2} \varepsilon \end{aligned} \quad (7)$$

and where $\bar{\Sigma}$ is the $d \times d$ correlation matrix of X , $\delta = (\delta(s_1), \dots, \delta(s_d))^\top$ and $D_\delta = \{1_d - \text{diag}(\delta^2)\}^{1/2}$, where 1_d is the identity matrix (Azzalini, 2013, Ch. 5). As a result, for any lag $h \in \mathbb{R}^k$, the distributions of $\{Z(s_1), \dots, Z(s_d)\}$ and $\{Z(s_1 + h), \dots, Z(s_d + h)\}$ will differ unless $\delta(s) = 0$ for all $s \in \mathbb{S}$. Hence, the distribution of Z is not translation invariant and the process is not strictly stationary. For $s \in \mathbb{S}$ and $h \in \mathbb{R}^k$, the mean $m(s)$ and covariance function $c_s(h)$ of the skew-normal random process are

$$m(s) = \mathbb{E}\{Z(s)\} = \delta(s)\phi(\varepsilon)/\Phi(\varepsilon)$$

and

$$c_s(h) = \text{Cov}\{Z(s), Z(s + h)\} = \rho(h)\sqrt{\{1 - \delta^2(s)\}\{1 - \delta^2(s + h)\}} + \delta(s)\delta(s + h)(1 - r), \quad (8)$$

where $r = \left\{ \frac{\phi(\varepsilon)}{\Phi(\varepsilon)} \left(\varepsilon + \frac{\phi(\varepsilon)}{\Phi(\varepsilon)} \right) \right\}$. Hence, the mean is not constant and that the covariance does not depend only on the lag h , unless $\delta(s) = \delta_0 \in (-1, 1)$ for all $s \in \mathbb{S}$. In the latter case the skew-normal random process is weakly stationary (Zhang and El-Shaarawi, 2010).

One benefit of working with a skew-normal random field is that the non-stationary covariance function (8) is positive definite if the covariance function of X is positive definite, and if $-1 < \delta(s) < 1$ for all $s \in \mathbb{S}$. Hence, a valid model is directly obtainable by means of standard parametric correlation models $\rho(h)$ and any bounded function δ in $(-1, 1)$. If the Gaussian process correlation function satisfies $\rho(0) = 1$ and $\rho(h) \rightarrow 0$ as $\|h\| \rightarrow +\infty$, then the correlation of the skew-normal process is

$$\rho_s(h) = \frac{c_s(h)}{\sqrt{c_s(0)c_s(h)}} \approx \frac{\delta(s)\delta(s + h)(1 - r)}{\sqrt{(1 - \delta^2(s)r)(1 - \delta^2(s + h)r)}},$$

as $\|h\| \rightarrow +\infty$, and $\rho_s(0) = 1$. Hence $\rho_s(h) = 0$ if either $\delta(s)$ or $\delta(s + h)$ are zero. Conversely, if both $\delta(s) \rightarrow \pm 1$ and $\delta(s + h) \rightarrow \pm 1$ then $\rho_s(h) \rightarrow \pm 1$.

The increments $Z(s + h) - Z(s)$ are skew-normal distributed for any $s \in \mathbb{S}$ and $h \in \mathbb{R}^k$ (see Appendix A.2) and the variogram $2\gamma_s(h) = \text{Var}\{Z(s + h) - Z(s)\}$ is equal to

$$2\gamma_s(h) = 2 \left(1 - c_s(h) - \frac{\delta^2(s + h) + \delta^2(s)}{\pi} \right).$$

When $h = 0$ the variogram is zero, and when $\|h\| \rightarrow +\infty$ the variogram approaches a constant ≤ 2 , resulting in spatial independence or dependence for large distances h . We can now infer the conditions required so that $Z(s)$ has a continuous sample path.

Proposition 2. *Assume that $\mathbb{S} \subseteq \mathbb{R}$. A skew-normal process $\{Z(s), s \in \mathbb{S}\}$ has a continuous sample path if $\delta(s + h) - \delta(s) = o(1)$ and $1 - \rho(h) = O(|\log|h||^{-a})$ for some $a > 3$, as $h \rightarrow 0$. Proof in Appendix A.2.*

This means that continuity of the skew-normal process is assured if $\delta(s)$ is a continuous function, in addition to the usual condition on the correlation function of the generating Gaussian process (e.g. Lindgren, 2012, Ch. 2).

Figure 1 illustrates trajectories of the skew-normal process for $k = 1$, with $X(s)$ a zero mean unit variance Gaussian process on $[0, 1]$ with isotropic power-exponential correlation function

$$\rho(h; \vartheta) = \exp\{-(h/\lambda)^\xi\}, \quad \vartheta = (\lambda, \xi), \quad \lambda > 0, \quad 0 < \xi \leq 2, \quad h > 0, \quad (9)$$

with $\xi = 1.5$, $\lambda = 0.3$ and $h \in [0, 1]$. The first row shows the standard stationary case. The second row illustrates the non-stationary correlation function obtained with $s = 0.1$ (solid line),

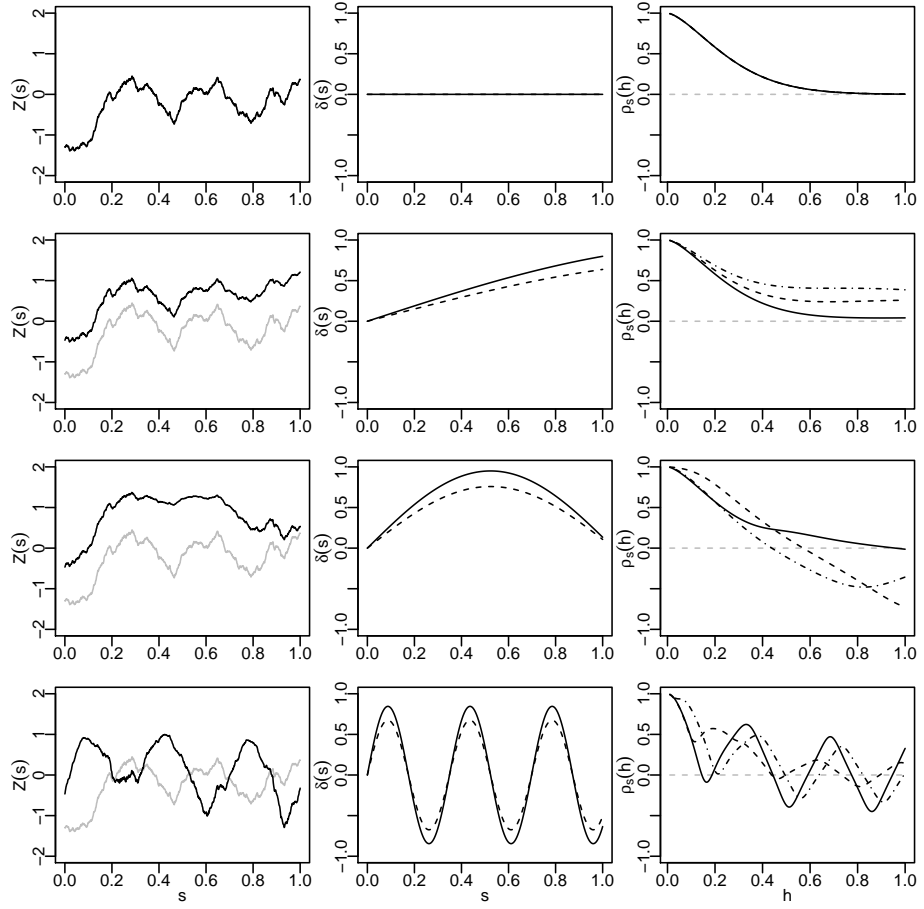


Figure 1: Simulations from four univariate skew-normal random processes on $[0, 1]$ with $\varepsilon = 0$. The left column shows the sample path (solid line) of the simulated process $Z(s)$ and of the generating Gaussian process $X(s)$ (grey line). The middle column illustrates the slant function $\delta(s)$ (solid line) and the mean $m(s)$ of the process (dashed line). The right column displays the non-stationary correlation functions at locations $s = 0.1$ (solid line), 0.5 and 0.75 (dot-dash). Rows 1–3 use slant function $\delta(s) = a \sin(bs)$ with $a = 0.95$ and $b = 0, 1$ and 3 respectively, whereas row 4 uses $\delta(s) = a^2 \sin(bs) \cos(bs)$ with $a = 1.3$ and $b = 0.9$.

close to the stationary correlation. Thus the correlation of the process at two locations s and $s+h$ vanishes asymptotically as $|h| \rightarrow +\infty$. The second row illustrates the non-stationary correlation function obtained with $s = 0.1$ (solid line) behaving close to the stationary correlation, with this correlation decaying more slowly as s increases (but not approaching zero). The third row demonstrates both that points may be negatively correlated and that $\rho_s(h)$ is not necessarily a decreasing function in h . The bottom row highlights this even more clearly – correlation functions need not be monotonically decreasing – implying that pairs of points far apart can be more dependent than nearby points.

Figure 2 displays an example of a bivariate ($k = 2$) anisotropic non-stationary correlation function $\rho_s(h)$. In the left panel, for any fixed direction from the origin, correlation decays monotonically with increasing distance, similar to the stationary case. However in the centre to right panels, the correlation function increasingly allows for the possibility that neighboring points can be less dependent than points far apart, for any fixed direction.

Simulating a skew-normal random process is computationally cheap through Definition 2, with the simulation of the required stationary Gaussian process achievable through many fast

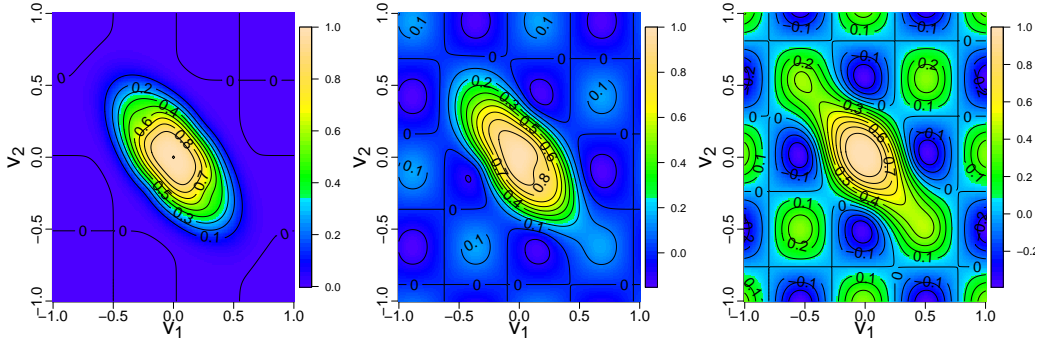


Figure 2: Bivariate geometric anisotropic non-stationary correlation functions $\rho_s(h)$, $s \in [0, 1]^2$ obtained using the slant function $\delta(s) = 0.9^2 \sin(6s_1) \cos(6s_2)$ and the correlation function (9) where $h = v^\top R v$, $v = (v_1, v_2)^\top \in [-1, 1]^2$, R being a matrix whose diagonal elements are 2.5 and those on the off-diagonal 1.5, $\xi = 1.5$ and $\lambda = 0.3$. From left to right, the points considered are respectively $s = (0.25, 0.5)^\top$, $(0.1, 0.1)^\top$ and $(0.8, 0.5)^\top$.

algorithms (e.g., Wood and Chan, 1994, Chan and Wood, 1997). Rather than relying on (7), for practical purposes, to directly simulate from a skew-normal process with given parameters α , $\bar{\Omega}$ and τ , a conditioning sampling approach can be adopted (Azzalini, 2013, Ch. 5).

Specifically, $X(s)$ define a zero-mean, unit variance stationary Gaussian random field on \mathbb{S} with correlation function $\omega(h) = \mathbb{E}\{X(s)X(s+h)\}$ and let $\bar{\Omega}$ be the $d \times d$ correlation matrix of $X(s_1), \dots, X(s_d)$. Specify $\alpha : \mathbb{S} \mapsto \mathbb{R}$ to be a continuous function for which the inner product $\langle \alpha, X \rangle = \int_{\mathbb{S}} \alpha(s)X(s) ds$ is available, and let X' be a standard normal random variable independent of X and $\tau \in \mathbb{R}$. If we define

$$Z(s) = \{X(s) | \langle \alpha, X \rangle > X' - \tau\}, \quad s \in \mathbb{S} \quad (10)$$

then, for any finite set $s_1, \dots, s_d \in \mathbb{S}$, the distribution of $Z(s_1), \dots, Z(s_d)$ is $\mathcal{SN}(\bar{\Omega}, \alpha, \tau)$, where $\alpha \equiv \{\alpha(s_1), \dots, \alpha(s_d)\}$. For simplicity we also refer to $\alpha(s)$ as the slant function. More efficient simulation of skew-normal processes can be achieved by considering the form $Z(s) = X(s)$ if $\langle \alpha, X \rangle > X' - \tau$ and $Z(s) = -X(s)$ otherwise (e.g. Azzalini, 2013, Ch. 5).

We now use these preliminary results to present our main contribution – the development of the extremal skew- t process.

3 Extremes of skew-symmetric data

3.1 Asymptotic behaviour

Consider $Z \sim \mathcal{SN}_d(\bar{\Omega}, \alpha)$, where $Z = \{Z(s_1), \dots, Z(s_d)\}^\top$ for a finite sequence of points $s_1, \dots, s_d \in \mathbb{S}$, with $d \geq 2$. Each margin $Z(s_i)$ follows a skew-normal distribution (Azzalini, 2013) and so is in the domain of attraction of a Gumbel distribution (Chang and Genton, 2007, Padoan, 2011). Further, each pair $(Z(s_i), Z(s_j))$ is asymptotically independent (Bortot, 2010, Lysenko et al., 2009) in the sense that the coefficient of upper tail dependence

$$\chi = \lim_{x \rightarrow +\infty} \Pr(Z(s_i) > x | Z(s_j) > x)$$

is equal to zero (e.g. Joe, 1997, Ch 5). This pairwise independence implies that Z is asymptotically independent (de Haan and Ferreira, 2006, Ch. 6), meaning that sample maxima become independent as $n \rightarrow \infty$. Similar conclusions hold for the lower tail.

Models that exhibit asymptotic independence can be useful for describing the joint behaviour of many extremal processes. If $Z = (Z_1, Z_2)^\top$ follows a bivariate distribution with unit-Fréchet margins, $\chi = 0$ does not necessarily imply that the joint upper tail decays to zero at the rate x^{-2} as $x \rightarrow +\infty$ (Ledford and Tawn, 1996). A broad class of tail behaviours can be obtained by assuming that the joint survival function is regularly varying at $+\infty$ with index $-1/\eta$ (Ledford and Tawn, 1996), so that

$$\Pr(Z_1 > x, Z_2 > x) = x^{-1/\eta} \mathcal{L}(x), \quad x \rightarrow +\infty, \quad (11)$$

where $\eta \in (0, 1]$ is the coefficient of tail dependence and $\mathcal{L}(x)$ is a slowly varying i.e., $\mathcal{L}(ax)/\mathcal{L}(x) \rightarrow 1$ as $x \rightarrow +\infty$, for fixed $a > 0$. Considering \mathcal{L} as a constant, at extreme levels random variables are negatively associated when $\eta < 1/2$, independent when $\eta = 1/2$ and positively associated when $1/2 < \eta < 1$. When $\eta = 1$ and $\mathcal{L}(x) \not\rightarrow 0$ asymptotic dependence is obtained.

We now derive the asymptotic behavior of the joint survival function (11) of the bivariate skew-normal distribution. As our primary interest is in spatial applications, we focus on the joint upper tail of the skew-normal distribution when the variables are positively correlated or uncorrelated.

Proposition 3. *Let $Z \sim \mathcal{SN}_2(\bar{\Omega}, \alpha)$, where $\alpha = (\alpha_1, \alpha_2)^\top$ and $\bar{\Omega}$ is a correlation matrix with off-diagonal term $\omega \in [0, 1)$. The joint survivor function of the bivariate skew-normal distribution with unit Fréchet margins behaves asymptotically as (11), where:*

1. when either $\alpha_1, \alpha_2 \geq 0$, or $\omega > 0$ and $\alpha_j \leq 0$ and $\alpha_{3-j} \geq -\omega^{-1}\alpha_j$ for $j = 1, 2$, then

$$\eta = (1 + \omega)/2, \quad \mathcal{L}(x) = \frac{2(1+\omega)}{1-\omega}(4\pi \log x)^{-\omega/(1+\omega)};$$

2. when $\omega > 0$, $\alpha_j < 0$, and $-\omega \alpha_j \leq \alpha_{3-j} < -\omega^{-1}\alpha_j$, for $j = 1, 2$, then

(a) If $\alpha_{3-j} > -\alpha_j/\bar{\alpha}_j$ then

$$\eta = \frac{(1-\omega^2)\bar{\alpha}_j^2}{1-\omega^2+(\bar{\alpha}_j-\omega)^2}, \quad \mathcal{L}(x) = \frac{2\bar{\alpha}_j^2(1-\omega^2)}{(\bar{\alpha}_j^2-\omega)(1-\omega\bar{\alpha}_j)}(4\pi \log x)^{1/2\eta-1};$$

(b) If $\alpha_{3-j} < -\alpha_j/\bar{\alpha}_j$ then

$$\eta = \left[\frac{1-\omega^2+(\bar{\alpha}_j-\omega)^2}{(1-\omega^2)\bar{\alpha}_j^2} + \left(\alpha_{3-j} + \frac{\alpha_j}{\bar{\alpha}_j} \right)^2 \right]^{-1},$$

$$\mathcal{L}(x) = \frac{-2^{3/2}\pi^{1/2}\bar{\alpha}_j^2(1-\omega^2)(\alpha_{3-j}+\alpha_j/\bar{\alpha}_j)^{-1}}{(\bar{\alpha}_j-\omega)\{1-\omega\bar{\alpha}_j+\alpha_j(\alpha_j+\alpha_{3-j}\bar{\alpha}_j)(1-\omega^2)\}}(4\pi \log x)^{1/2\eta-3/2};$$

3. when either $\alpha_1, \alpha_2 < 0$, or $\omega > 0$, $\alpha_j < 0$ and $0 < \alpha_{3-j} < -\omega \alpha_j$ for $j = 1, 2$, then

$$\eta = \left\{ \frac{1}{1-\omega^2} \left(\frac{\alpha_{3-j}^2(1-\omega^2)+1}{\bar{\alpha}_{3-j}^2} + \frac{\alpha_j^2(1-\omega^2)+1}{\bar{\alpha}_j^2} + \frac{2(\alpha_{3-j}\alpha_j(1-\omega^2)-\omega)}{\bar{\alpha}_{3-j}\bar{\alpha}_j} \right) \right\}^{-1},$$

$$\mathcal{L}(x) = \frac{-2^{3/2}\pi^{1/2}\bar{\alpha}_j^{3/2}\bar{\alpha}_{3-j}^2(1-\omega^2)(\alpha_i\bar{\alpha}_j+\alpha_j\bar{\alpha}_{3-j})^{-1}}{(\bar{\alpha}_j-\omega\bar{\alpha}_{3-j})\{1-\omega\bar{\alpha}_j+\alpha_j(\alpha_j+\alpha_{3-j}\bar{\alpha}_j/\bar{\alpha}_{3-j})(1-\omega^2)\}}(4\pi \log x)^{1/2\eta-3/2};$$

where $\bar{\alpha}_j = \sqrt{1 + \alpha_j^{*2}}$ and $\alpha_j^* := \alpha_{\{j\}}^* = \frac{\alpha_j + \omega\alpha_{3-j}}{\sqrt{1 + \alpha_{3-j}(1 - \omega^2)}}$.

Proof in Appendix A.3.

As a result, when both marginal parameters are non-negative (case 1) then $1/2 \leq \eta < 1$, with $\eta = 1/2$ occurring when $\omega = 0$. As a consequence, as for the Gaussian distribution (for which $\alpha = 0$) the marginal extremes are either positively associated or exactly independent. The marginal extremes are also completely dependent when $\omega = 1$, regardless of the values of the slant parameters, α . When one marginal parameter is positive and one is negative (case 2) then $\eta > (1 + \omega)/2$. In this case the extreme marginals are also positively associated, but the dependence is greater than when the random variables are normally distributed. Finally, when both marginal parameters are negative (case 3), then $0 < \eta < 1/2$ implying that the extreme marginals are negatively associated, although $\omega > 0$. It should be noted that differently from the Gaussian case ($\alpha = 0$) where $\omega > 0$ implies a positive association, in this case it is not necessary true. In summary, the degree of dependence in the upper tail of the skew-normal distribution ranges from negative to positive association and including independence.

The skew- t distribution is known to exhibit asymptotic dependence in both upper and lower tails, with a different coefficient of tail dependence for each tail (Padoan, 2011). It is accordingly more flexible than the symmetric t distribution which possesses identical coefficients for each tail. We conclude this section by showing that the tail behaviour of the non-central extended skew- t distribution in Definition 1 is the same as the standard skew- t distribution discussed in (Padoan, 2011).

Proposition 4. *Let Z_1, \dots, Z_n be iid copies of $Z \sim \mathcal{ST}_d(\bar{\Omega}, \alpha, \tau, \kappa, \nu)$ and M_n be the componentwise sample maxima. Define $a_n = (a_{n,1}, \dots, a_{n,d})^\top$, where*

$$a_{n,j} = \left\{ \frac{n\{\Gamma(\nu/2)\}^{-1}\Gamma\{(\nu+1)/2\}\nu^{(\nu-2)/2}\Psi(\alpha_j^*\sqrt{\nu+1}; \kappa, \nu+1)}{\sqrt{\pi}\Psi\left(\tau_j^*/\{1+Q_{\bar{\Omega}}(\alpha_j^*)\}^{1/2}; \kappa_j^*/\{1+Q_{\bar{\Omega}}(\alpha_j^*)\}, \nu\right)} \right\}^{1/\nu}$$

where $\alpha_j^* = \alpha_{\{j\}}^*$, $\tau_j^* = \tau_{\{j\}}^*$ and $\kappa_j^* = \kappa_{\{j\}}^*$ are the marginal parameters (5) under Proposition 1(1). Then $M_n/a_n \Rightarrow U$ as $n \rightarrow +\infty$, where U has univariate ν -Fréchet marginal distributions (i.e. $e^{-x^{-\nu}}$, $x > 0$), and exponent function

$$V(x_j, j \in I) = \sum_{j=1}^d x_j^{-\nu} \Psi_{d-1} \left(\left(\sqrt{\frac{\nu+1}{1-\omega_{i,j}^2}} \left(\frac{x_i^+}{x_j^+} - \omega_{i,j} \right), i \in I_j \right)^\top; \bar{\Omega}_j^+, \alpha_j^+, \tau_j^+, \nu+1 \right), \quad (12)$$

where Ψ_{d-1} is a $(d-1)$ -dimensional central extended skew- t distribution with correlation matrix $\bar{\Omega}_j^+$, shape and extension parameters α_j^+ and τ_j^+ , and $\nu+1$ degrees of freedom, $I = \{1, \dots, d\}$, $I_j = I \setminus \{j\}$, and $\omega_{i,j}$ is the (i, j) -th element of $\bar{\Omega}$.

Proof (and further details) in Appendix A.4.

As the limiting distribution (12) is the same as that of the classic skew- t distribution (see Padoan, 2011), it exhibits identical upper and lower tail dependence coefficients (e.g. Joe, 1997, Ch 5). That is, the extension and non-centrality parameters, τ and κ , do not affect the extremal behavior.

3.2 Spectral representation for the extremal-skew- t process

The spectral representation of stationary max-stable processes with common unit Fréchet margins can be constructed using the fundamental procedures introduced by de Haan (1984) and Schlather (2002) (see also de Haan and Ferreira, 2006, Ch. 9). This representation can be formulated in broader terms resulting in max-stable processes with ν -Fréchet univariate marginal

distributions, with $\nu > 0$ Opitz (2013). In order to state our result we rephrase the spectral representation so to also take into account non-stationary processes.

Let $\{Y(s)\}_{s \in \mathbb{S}}$ be a non-stationary real-valued stochastic process with continuous sample path on \mathbb{S} such that $\mathbb{E}\{\sup_{s \in \mathbb{S}} Y(s)\} < \infty$ and $m^+(s) = \mathbb{E}\{Y^+(s)\}^\nu < \infty, \forall s \in \mathbb{S}$ for $\nu > 0$, where $Y^+(\cdot) = \max\{Y(\cdot), 0\}$ denotes the positive part of Y . Let $\{R_i\}_{i \geq 1}$ be the points of an inhomogeneous Poisson point process on $(0, \infty)$ with intensity $\nu r^{-(\nu+1)}$, $\nu > 0$, which are independent of Y . Define

$$U(s) = \max_{i=1,2,\dots} \{R_i Y_i^+(s)\} / \{m^+(s)\}^{1/\nu}, \quad s \in \mathbb{S}, \quad (13)$$

where Y_1, Y_2, \dots are *iid* copies of Y . Then U is a max-stable process with common ν -Fréchet univariate margins. In particular, for fixed $s \in \mathbb{S}$ and $x(s) > 0$ we have

$$\Pr(U(s) \leq x(s)) = \exp \left[-\frac{\mathbb{E}\{Y^+(s)\}^\nu}{x^\nu(s)m^+(s)} \right] = \exp\{-1/x^\nu(s)\},$$

and for fixed s_1, \dots, s_d the finite dimensional distribution of U has exponent function

$$V(x(s_1), \dots, x(s_d)) = \mathbb{E} \left(\max_j \left[\frac{\{Y^+(s_j)/x(s_j)\}^\nu}{m^+(s_j)} \right] \right), \quad x(s_j) > 0, j = 1, \dots, d \quad (14)$$

(de Haan and Ferreira, 2006, Ch. 9).

In this construction, the impact of a non-stationary process $Y(s)$ would be that the dependence structure of the max-stable process $U(s+h)$ depends on both the separation h and the location $s \in \mathbb{S}$, and would therefore itself be non-stationary. The below theorem derives a max-stable process $U(s)$ when $Y(s)$ is the skew-normal random field introduced in Section 2.2.

Theorem 1 (Extremal skew- t process). *Let $Y(s)$ be a skew-normal random field on $s \in \mathbb{S}$ with finite dimensional distribution $\mathcal{SN}_d(\bar{\Omega}, \alpha, \tau)$, as defined in equation (10). Then the max-stable process $U(s)$, given by (13), has ν -Fréchet univariate marginal distributions and exponent function*

$$V(x_j, j \in I) = \sum_{j=1}^d x_j^{-\nu} \Psi_{d-1} \left(\left(\sqrt{\frac{\nu+1}{1-\omega_{i,j}^2}} \left(\frac{x_i^\circ}{x_j^\circ} - \omega_{i,j} \right), i \in I_j \right)^\top; \bar{\Omega}_j^\circ, \alpha_j^\circ, \tau_j^\circ, \kappa_j^\circ, \nu+1 \right), \quad (15)$$

where $x_j \equiv x(s_j)$, Ψ_{d-1} is a $(d-1)$ -dimensional non-central extended skew- t distribution (Definition 1) with correlation matrix $\bar{\Omega}_j^\circ$, shape, extension and non-centrality parameters $\alpha_j^\circ, \tau_j^\circ$ and κ_j° , $\nu+1$ degrees of freedom, $I = \{1, \dots, d\}$, $I_j = I \setminus \{j\}$, and $\omega_{i,j}$ is the (i, j) -th element of $\bar{\Omega}$.

Proof (and further details) in Appendix A.5.

We call the process $U(s)$ with exponent function (15) an extremal skew- t process.

Note that in Theorem 1 when $\tau = 0$, and the slant function is such that $\alpha(s) \equiv 0$ for all $s \in \mathbb{S}$, then the exponent function (15) becomes

$$V(x_j, j \in I) = \sum_{j \in I} x_j^{-\nu} \Psi_{d-1} \left[\left(\sqrt{\frac{\nu+1}{1-\omega_{i,j}^2}} \left(\frac{x_i}{x_j} - \omega_{i,j} \right), i \in I_j \right)^\top; \bar{\Omega}_j^\circ, \nu+1 \right]. \quad (16)$$

This is the exponent function of the extremal- t process as discussed in Opitz (2013).

If we assume $\tau = 0$ in (10), then the bivariate exponent function of the extremal skew- t process seen as a function of the separation h is equal to

$$V\{x(s), x(s+h)\} = \frac{\Psi(b(x_s^*(h)); \alpha_s^*(h), \tau_s^*(h), \nu+1)}{x^\nu(s)} + \frac{\Psi(b(x_s^+(h)); \alpha_s^+(h), \tau_s^+(h), \nu+1)}{x^\nu(s+h)}$$

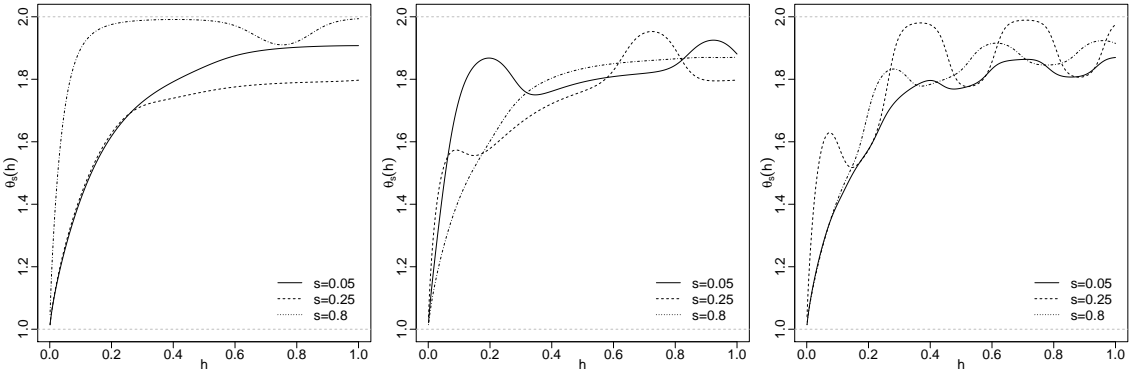


Figure 3: Examples of univariate ($k = 1$) non-stationary isotropic extremal coefficient functions $\theta_s(h)$, for the extremal skew- t process over $s \in [0, 1]$, using correlation function (9) where $h \in [0, 1]$, $\lambda = 1.5$ and $\gamma = 0.3$. Slant functions are (left to right panels): $\alpha(s) = -1 - s + \exp\{\sin(5s)\}$, $\alpha(s) = 1 + 1.5s - \exp\{\sin(8s)\}$ and $\alpha(s) = 2.25 \sin(9s) \cos(9s)$. Solid, dashed and dot-dashed lines represent the fixed locations $s = 0.05, 0.25$ and 0.8 respectively.

where Ψ is a univariate extended skew- t distribution, $b(\cdot) = \sqrt{\frac{\nu+1}{1-\omega^2(h)}}(\cdot - \omega(h))$,

$$\begin{aligned} x_s^*(h) &= \frac{x(s+h)\Gamma_s(h)}{x(s)}, & x_s^+(h) &= \frac{x(s)}{x(s+h)\Gamma_s(h)}, \\ \alpha_s^*(h) &= \alpha(s+h)\sqrt{1-\omega^2(h)}, & \alpha_s^+(h) &= \alpha(s)\sqrt{1-\omega^2(h)}, \\ \tau_s^*(h) &= \sqrt{\nu+1}\{\alpha(s) + \alpha(s+h)\omega(h)\}, & \tau_s^+(h) &= \sqrt{\nu+1}\{\alpha(s+h) + \alpha(s)\omega(h)\}, \end{aligned}$$

and

$$\Gamma_s(h) = \left(\frac{\Psi \left[\alpha(s) + \alpha(s+h)\omega(h) \sqrt{\frac{\nu+1}{\alpha^2(s+h)\{1-\omega^2(h)\}}}; \nu+1 \right]}{\Psi \left[\alpha(s+h) + \alpha(s)\omega(h) \sqrt{\frac{\nu+1}{\alpha^2(s)\{1-\omega^2(h)\}}}; \nu+1 \right]} \right)^{1/\nu}.$$

Clearly, as the dependence structure depends on both correlation function $\omega(h)$ and the slant function $\alpha(s)$, and therefore on the value of $s \in \mathbb{S}$, it is a non-stationary dependence structure. From the bivariate exponent function we can derive the non-stationary extremal coefficient function, using the relation $\theta_s(h) = V(1, 1)$, which gives

$$\theta_s(h) = \Psi(b(\Gamma_s(h)); \alpha_s^*(h), \tau_s^*(h), \nu+1) + \Psi(b(1/\Gamma_s(h)); \alpha_s^+(h), \tau_s^+(h), \nu+1) \quad (17)$$

Figure 3 shows some examples of univariate ($k = 1$) non-stationary isotropic extremal coefficient functions obtained from (17) using the power-exponential correlation function (9). Each panel illustrates a different slant function $\alpha(s)$, with the line-types indicating the fixed location value of $s \in \mathbb{S}$. The extremal coefficient functions $\theta_s(h)$ increase as the value of h increases, meaning that the dependence of extremes decreases with the distance. $\theta_s(h)$ grows with different rates depending on the location $s \in \mathbb{S}$. Although the ergodicity and mixing properties of the process must be investigated, numerical results show that for some s , $\theta_s(h) \rightarrow 2$ as $|h| \rightarrow +\infty$. By increasing the complexity of the slant function (e.g. centre and right panels) it is possible to construct extremal coefficient functions which exhibit stronger dependence for larger distances, h , compared to shorter distances. Similarly Figure 4 illustrates examples of bivariate ($k = 2$) non-stationary geometric anisotropic extremal coefficient functions, $\theta_s(h)$, also obtained from

(17). The examples are under the same settings as for Figure 2, but using different slant functions and fixed locations $s \in \mathbb{S}$. Similar interpretations to the univariate case can be made (Figure 3), in addition to noting that the level of dependence is affected by the direction (from the origin).

3.3 Angular density of the extremal-skew- t model

The angular measure of the extremal-skew- t dependence model (15) places mass on the interior as well as on the other subspaces of the simplex, such as the edges and the vertices. Therefore, different angular densities lie on these sets. We derive these densities following Coles and Tawn (1991).

Let J be an index set that takes values in $\mathbb{I} = \mathbb{P}(\{1, \dots, d\}) \setminus \emptyset$, where $\mathbb{P}(I)$ is the power set of I . For any fixed d and all $J \in \mathbb{I}$, the sets

$$\mathbb{W}_{d,J} = (w \in \mathbb{W} : w_j = 0, \text{ if } j \notin J; w_j > 0 \text{ if } j \in J)$$

provide a partition of the d -dimensional simplex \mathbb{W} into $2^d - 1$ subsets. Let $k = |J|$ be the size of J . Let $h_{d,J}$ denote the density that lies on the subspace $\mathbb{W}_{d,J}$, which has $k - 1$ free parameters w_j such that $j \in J$. When $J = \{1, \dots, d\}$ and when the joint distribution (1), with common unit Fréchet margins, is absolutely continuous, the angular density in the interior of the simplex

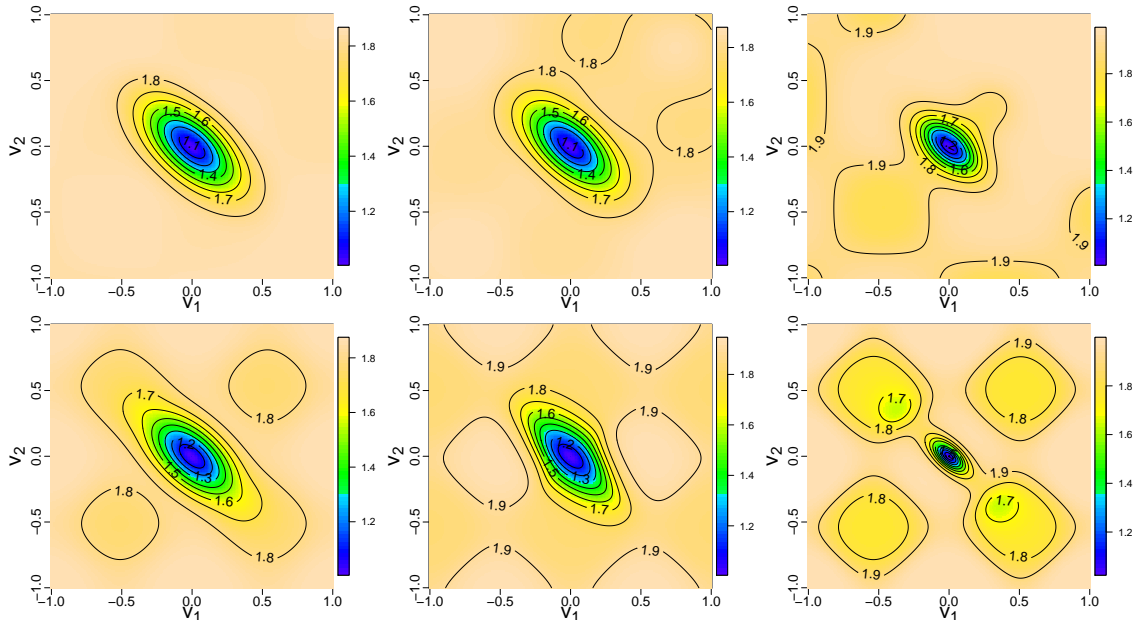


Figure 4: Bivariate ($k = 2$) geometric anisotropic non-stationary extremal coefficient functions $\theta_s(h)$, for the extremal skew- t process on $s \in [0, 1]^2$, based on extremal coefficient function (17) with $\lambda = 1.5$ and $\gamma = 0.3$, where $h = v^\top R v$, $v = (v_1, v_2)^\top \in [-1, 1]^2$ and R is a 2×2 matrix whose diagonal elements are 2.5 and off-diagonal elements 1.5. Slant functions are $\alpha(s) = \exp\{\sin(4s_1)\sin(4s_2) - s_1s_2 - 1\}$ (top panels) and $\alpha(s) = 2.25\{\sin(3s_1)\cos(3s_1) + \sin(3s_2)\cos(3s_2)\}$ (bottom), with $s = (s_1, s_2)^\top \in [0, 1]^2$. Left to right, panels are based on fixing $s = (0.2, 0.2)^\top$, $s = (0.4, 0.4)^\top$ and $s = (0.85, 0.85)^\top$ (top panels) and $s = (0.25, 0.25)^\top$, $s = (0.25, 0.8)^\top$ and $s = (0.8, 0.8)^\top$ (bottom).

is

$$h(w) = \frac{\psi_{d-1} \left(\left[\sqrt{\frac{\nu+1}{1-\omega_{i,1}^2}} \left\{ \left(\frac{w_i^\circ}{w_1^\circ} \right)^{1/\nu} - \omega_{i,1} \right\}, i \in I_1 \right]^\top; \Omega_1^\circ, \alpha_1^\circ, \tau_1^\circ, \kappa_1^\circ, \nu + 1 \right)}{w_1^{(d+1)} \left\{ \prod_{i=2}^d \frac{1}{\nu} \sqrt{\frac{\nu+1}{1-\omega_{i,1}^2}} \left(\frac{w_i^\circ}{w_1^\circ} \right)^{\frac{1}{\nu}-1} \frac{m_i^+}{m_1^+} \right\}^{-1}}, \quad w \in \mathbb{W} \quad (18)$$

where ψ_{d-1} denotes the $d-1$ -dimensional skew- t density, $I_j = \{1, \dots, d\} \setminus j$ and where the parameters $\Omega_1^\circ, \alpha_1^\circ, \tau_1^\circ, \kappa_1^\circ$ and $w_i^\circ = x_i(m_i^+)^{1/\nu}$ are given in the proof to Theorem 1 (Appendix A.5). When $J = \{i_1, \dots, i_k\} \subset \{1, \dots, d\}$, the angular density for any $x \in \mathbb{R}_+^d$ is

$$h_{d,J} \left(\frac{x_{i_1}}{\sum_{i \in J} x_i}, \dots, \frac{x_{i_{k-1}}}{\sum_{i \in J} x_i} \right) = - \left(\sum_{i \in J} x_i \right)^{k+1} \lim_{\substack{x_j \rightarrow 0, \\ j \notin J}} \frac{\partial^k V}{\partial x_{i_1} \cdots \partial x_{i_k}}(x). \quad (19)$$

When $J = \{j\}$ for any $j \in \{1, \dots, d\}$ then $\mathbb{W}_{d,J}$ is a vertex \mathbf{e}_j of the simplex and the density is a point mass, denoted $h_{d,J} = H(\{\mathbf{e}_j\})$. In this case (19) reduces to

$$H(\{\mathbf{e}_j\}) = \Psi_{d-1} \left\{ \left(-\sqrt{\frac{\nu+1}{1-\omega_{i,j}^2}} \omega_{i,j}, i \in I_j \right)^\top; \Omega_j^\circ, \alpha_j^\circ, \tau_j^\circ, \kappa_j^\circ, \nu + 1 \right\}, \quad (20)$$

where Ψ_{d-1} denotes the $d-1$ -dimensional skew- t distribution with parameters again given in the proof to Theorem 1 (Appendix A.5).

Practically, computation of all $2^d - 1$ densities that lie on the edges and vertices of the simplex is not feasible for $d > 3$ dimensions, however, the calculations are viable for $d = 3$. Let $J = \{1, 2, 3\}$. The angular densities that lie on the interior and vertices of the simplex can be derived from (18) and (20). For all $i, j \in J$, with $i \neq j$, the angular density that lies on the edges of $\mathbb{W}_{d,J}$ for $w \in \mathbb{W}_{d,J}$ is given by

$$\begin{aligned} h_{3,\{i,j\}}(w) &= \sum_{u,v \in \{i,j\}, u \neq v} \left(\frac{\psi(b_{u,v}^\circ; \nu + 1)}{\Psi(\bar{\tau}_u; \nu + 1)} \Psi_2 \left[\{y_1^\circ(u, v), y_2^\circ(u, v)\}^\top; \bar{\Omega}_u^{\circ\circ}, \nu + 2 \right] \right. \\ &\quad \times \frac{1}{w_1} \left\{ \frac{d^2 b_{u,v}^\circ}{dw_u dw_v} + \frac{db_{u,v}^\circ}{dw_v} \left(\frac{db_{u,v}^\circ}{dw_u} \frac{(\nu + 2)b_{u,v}^\circ}{\nu + 1 + b_{u,v}^{\circ 2}} - \frac{1}{w_1} \right) \right\} \\ &\quad + \psi\{y_1^\circ(u, v); \nu + 2\} \sqrt{\frac{\nu + 2}{1 - \Omega_{u,[1,2]}^{\circ 2}}} \frac{b_{u,v}^\circ c_{u,\bar{k}} + \Omega_{u,[1,2]}^{\circ 2}(\nu + 1)}{(\nu + 1 + b_{u,v}^{\circ 2})^{3/2}} \\ &\quad \times \Psi \left(\frac{\sqrt{\nu + 3} \left\{ z_2^\circ(u, v) \Omega_{u,[1,1]}^{\circ\circ} - z_1^\circ(u, v) \Omega_{u,[1,2]}^{\circ\circ} \right\}}{\sqrt{\left[\Omega_{u,[1,1]}^{\circ\circ} \{\nu + 1 + b_{u,v}^{\circ 2}\} + z_1^{\circ 2}(u, v) \right] \det(\Omega_u^{\circ\circ})}}; \nu + 3 \right) \quad (21) \\ &\quad + \psi\{y_2^\circ(u, v); \nu + 2\} \sqrt{\frac{\nu + 2}{1 - \Omega_{u,[1,3]}^{\circ 2}}} \frac{x(u, v) \bar{\tau}_u + \Omega_{u,[1,3]}^{\circ 2}(\nu + 1)}{\{\nu + 1 + b_{u,v}^{\circ 2}\}^{3/2}} \\ &\quad \times \Psi \left(\frac{\sqrt{\nu + 3} \left\{ z_1^\circ(u, v) \Omega_{u,[2,2]}^{\circ\circ} - z_2^\circ(u, v) \Omega_{u,[1,2]}^{\circ\circ} \right\}}{\sqrt{\left(\Omega_{u,[2,2]}^{\circ\circ} \{\nu + 1 + b_{u,v}^{\circ 2}\} + z_2^{\circ 2}(u, v) \right) \det(\Omega_u^{\circ\circ})}}; \nu + 3 \right) \end{aligned}$$

where for all $u, v \in J$, with $u \neq v$, and $\bar{k} \notin \{i, j\}$,

$$y_\ell^\circ(u, v) = \frac{z_\ell^\circ(u, v)}{\sqrt{\Omega_{u,[\ell,\ell]}^\circ}} \sqrt{\frac{\nu + 2}{\nu + 1 + b_{u,v}^{\circ 2}}}, \quad \ell = 1, 2, \quad z_1^\circ(u, v) = c_{u,\bar{k}} - \Omega_{u,[1,2]}^\circ b_{u,v}^\circ, \\ c_{u,v} = -\omega_{u,v} \sqrt{\frac{\nu + 1}{1 - \omega_{u,v}^2}}, \quad z_2^\circ(u, v) = \bar{\tau}_u - \Omega_{u,[1,3]}^\circ, \quad b_{u,v}^\circ, \quad \Omega_u^\circ = \begin{bmatrix} \bar{\Omega}_u & -\delta_u \\ -\delta_u^\top & 1 \end{bmatrix}, \\ \delta_u^\top = \bar{\Omega}_u \left(\alpha_v \sqrt{1 - \omega_{u,v}^2}, \alpha_k \sqrt{1 - \omega_{u,k}^2} \right)^\top, \quad \bar{\Omega}_u^{\circ\circ} = \omega_u^{\circ -1/2} \Omega_u^{\circ\circ} \omega_u^{\circ -1/2},$$

$\omega_u^\circ = \text{diag}(\Omega_u^{\circ\circ})$, $\Omega_u^{\circ\circ} = \Omega_{u,[-1,-1]}^\circ - \Omega_{u,[-1,1]}^\circ \Omega_{u,[1,-1]}^\circ$. Components of Ω_u° and $\Omega_u^{\circ\circ}$ are respectively given by $\Omega_{u,[i,j]}^\circ$ and $\Omega_{u,[i,j]}^{\circ\circ}$ for $i, j \in J$. See also Appendix A.5 for further details.

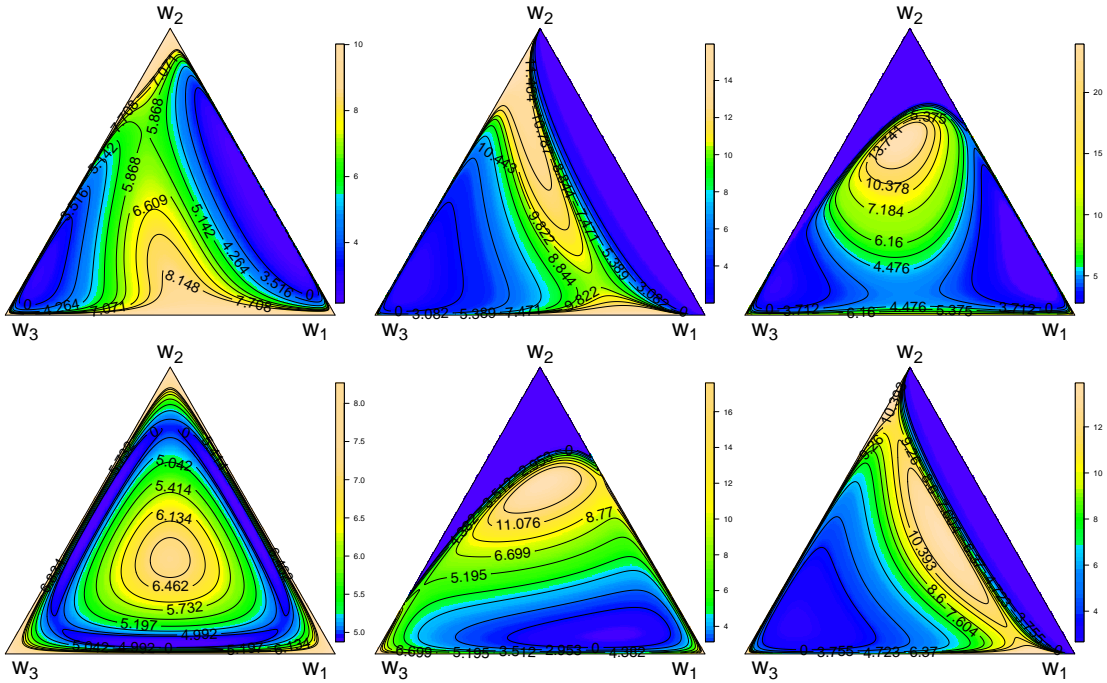


Figure 5: Trivariate extremal skew- t angular densities with $\nu = 2$ degrees of freedom. Correlation coefficients are $\omega = (0.52, 0.71, 0.52)^\top$ for the top row and $\omega = (0.95, 0.95, 0.95)^\top$ for the bottom. Left and centre columns respectively have skewness $\alpha = (0, 0, 0)^\top$ and $\alpha = (-2, -2, 5)^\top$. Right column has $\alpha = (-10, 5, 1)^\top$ (top) and $\alpha = (-2, -2, -2)^\top$ (bottom). In all cases $\tau = 0$ for simplicity.

When the extension and slant parameters are null ($\tau = 0, \alpha(s) = 0$), then the densities (18), (20) and (21) reduce to the densities of the extremal- t angular measure. Figure 5 illustrates some examples of the flexibility of the trivariate extremal-skew- t dependence structure. Here we write the correlation coefficients as $\omega = (\omega_{1,2}, \omega_{1,3}, \omega_{2,3})^\top$ and the slant parameters as $\alpha = (\alpha_{1,2}, \alpha_{1,3}, \alpha_{2,3})^\top$, and assume that $\nu = 2$ and $\tau = 0$ for simplicity.

The plots in the left column have $\alpha = (0, 0, 0)^\top$ and so correspond to the extremal- t angular measure. The density in the top-left panel, obtained with $\omega = (0.52, 0.71, 0.52)^\top$, has mass concentrations mainly on the edge that links the first and the third variable, since they are the most dependent ($w_{1,3} = 0.71$). Some mass is also placed on the corners of the second variable, indicating that this is less dependent on the others ($w_{1,2} = w_{2,3} = 0.52$), and on the middle of the simplex, because a low degree of freedom ($\nu = 2$) pushes mass towards the centre of the simplex. The top-middle and top-right panels are extremal skew- t angular densities obtained

with $\alpha = (-2, -2, 5)^\top$ and $\alpha = (-10, 5, 1)^\top$ respectively. Here the impact of the slant parameter is to increase the levels of dependence – indeed the mass is clearly pushed towards the centre of the simplex. In the middle panel dependence between the second and third variables has increased, while in the right panel all variables are strongly dependent with a greater dependence of the second variable on the others.

The bottom row in Figure 5 illustrates the spectral densities with correlation coefficients $\omega = (0.95, 0.95, 0.95)^\top$. The bottom-left panel is the standard extremal- t dependence (with $\alpha = (0, 0, 0)^\top$), which has a symmetric density with mass concentrated mainly in the centre of the simplex and on the vertices. The top-middle and top-right panels show extremal skew- t densities, obtained with $\alpha = (-2, -2, 5)^\top$ and $\alpha = (-2, -2, -2)^\top$ respectively. In this case the impact of the slant parameter is to decrease the dependence – here the mass is pushed towards the edges of the simplex. In the middle panel the second variable has become more dependent on the others, while in the right panel the third variable is more dependent on the others. These examples illustrate the great flexibility of the extremal skew- t model in capturing a wide range of extremal dependence behaviour above and beyond that of the standard extremal t model.

4 Inference

4.1 Composite and approximate likelihoods

The density function of the extremal-skew- t process is practically infeasible to compute for a large number of locations d . However, it is viable to derive all marginal densities for up to $d = 4$ dimensions. The forms of these marginal densities for $d = 2, 3, 4$ are provided in Appendix B.1. Given these, the dependence parameters of the process can then be estimated using composite-likelihood approaches (e.g. Padoan et al., 2010, Davison and Gholamrezaee, 2012, Huser and Davison, 2013).

Let $\vartheta \in \Theta$ denote the vector of dependence parameter of the extremal-skew- t process. Consider a sample $x_1, \dots, x_n \in \mathbb{R}_+^d$ of n iid replicates of the process observed over a finite number of points $s_1, \dots, s_d \in \mathbb{S}$. For simplicity, it is assumed that the univariate marginal distributions are unit Fréchet. The pairwise ($m = 2$) or triplewise ($m = 3$) log-composite-likelihood is defined by

$$\ell_m(\vartheta; x) = \sum_{i=1}^n \sum_{E \in E_m} \log f(x_i \in E; \vartheta), \quad m = 2, 3,$$

where $x = (x_1, \dots, x_n)^\top$ and f is a marginal extremal-skew- t probability density function associated with each member of a set of marginal events E_m . See e.g. Varin et al. (2011) for a complete description of composite likelihood methods.

An alternative to full-likelihood estimation is the approximate likelihood approach introduced by Coles and Tawn (1994), which is constructed on the space of angular densities. Angular densities for the extremal-skew- t dependence model were derived in Section 3.3. In particular for $d = 3$, all densities lying on the interior, edges and vertices of the simplex were derived, and so estimation based on the approximate-likelihood method is feasible for this case.

Consider the set of observations $\{(r_i, w_i) : i = 1, \dots, n\}$ where $r_i = x_{i,1} + \dots + x_{i,d}$ and $w_i = x_i/r_i$ are pseudo-polar radial and angular components. Then the approximate log-likelihood is defined by

$$\ell(\vartheta; w) = \sum_{\substack{i=1, \dots, n: \\ r_i > r_0}} \log h(w_i; \vartheta), \quad (22)$$

where $w = (w_1, \dots, w_n)^\top$, for some radial threshold $r_0 > 0$, where h is the angular density function of the extremal-skew- t dependence model. As the angular measure of the extremal-skew- t process places mass on all the subspaces of the simplex, all such densities must be adopted in the log-likelihood (22).

4.2 Simulation Study

We consider two specific simulations. Firstly, we demonstrate that in the $d = 3$ dimensional case, the parameters of the extremal- t dependence model (16) can be reliably estimated using the approximate-likelihood (22). A similar study has been performed by Thibaud and Optiz (2015). Secondly, we perform a simulation study related to that of Huser and Davison (2013), and demonstrate that the triplewise maximum-likelihood estimator can be more efficient than the pairwise maximum-likelihood estimator for the extremal- t process.

In the first case we estimate the correlation parameters $\omega = (\omega_{1,2}, \omega_{1,3}, \omega_{2,3})^\top$ while fixing ν for simplicity. For each combination of parameter vectors $\omega = (0.6, 0.8, 0.7)^\top, (0.7, 0.7, 0.7)^\top$ and $(0.2, 0.8, 0.5)^\top$ and degrees of freedom $\nu = 1, 3$ and 4 , 1000 replicate datasets of 500 observations are simulated and transformed to pseudo-polar coordinates. In each case the $n = 100$ observations with the largest radial component are retained. For each angular component $w_1, \dots, w_n \in \mathbb{W}_{3,I}$ where $I = \{1, 2, 3\}$, the angular density used in (22) is established by defining a small threshold $c \geq 0$. When $w_{i,j} > c$ for all $j \in I$, then w_i falls in the interior of the simplex and so we use (18). When $w_{i,j} \leq c$ for one $j \in I$, then w_i falls on the edge that links $w_{i,k}$ and $w_{i,\ell}$, where $k \neq \ell \in I \setminus \{j\}$, and so we use (21). Finally, when $w_{i,\ell} > c$ for only one $\ell \in I$, then w_i falls on the vertex of the ℓ^{th} component, and the angular density is given as (20).

Figure 6 displays the resulting mean of the 1000 maximum approximate likelihood estimates (solid lines) as the small threshold c varies in $[0, 0.1]$. Red, green and blue lines correspond to the three known parameter vectors ω above, where dashed lines indicate the true values. Columns correspond to the different parameters $\omega_{i,j}$, and rows to the varying (but fixed) degrees of freedom ν . It is immediately apparent that if the approximate likelihood (22) does not include sub-densities that lie on the edges (21) and vertices (20) of the simplex, so that for $c = 0$ all observations w_i are assumed to lie on the interior of the simplex regardless of the size of each $w_{i,j}$, then the parameters are overestimated. Similarly, if the threshold c is too large, then too many w_i are allocated to edge and vertex densities rather than the interior of the simplex, and so the parameters are underestimated.

The optimum choice of threshold seems to be around $c = 0.1, 0.06$ and 0.05 for strong ($\nu = 1$), moderate ($\nu = 3$) or weak dependence ($\nu = 4$) respectively, indicating that greater dependence requires an increased allocation of w_i to edge or vertex densities. A smaller effect occurs in relation to the size of $\omega_{i,j}$ in that a lower threshold c is required to reliably estimate $\omega_{i,j}$ when the true value is small compared to if the true value is large (this is most clearly seen in the left column of Figure 6). This last point suggests that if the true $\omega_{i,j}$ are very different from each other (e.g. consider the blue lines in the bottom row of Figure 6), then there is no single threshold c that can yield accurate estimates over all parameters, and that parameter specific thresholds may be required.

We repeat this study for different sample sizes $n = 50, 100, 500$ (achieved by varying the radial threshold r_0), and compare the results with those obtained using the pairwise composite likelihood and the full likelihood (see Appendix B.1 for the derivation of the required densities for $d = 2, 3$). The results are presented in Table 1, which for brevity reports the results for $\omega = (0.6, 0.8, 0.7)^\top$ and $\nu = 3$ only (similar results are achieved in the other parameter settings).

Clearly, the estimates obtained with the pairwise composite likelihood are very similar to those obtained using the full-likelihood. In comparison, the estimates obtained using the ap-

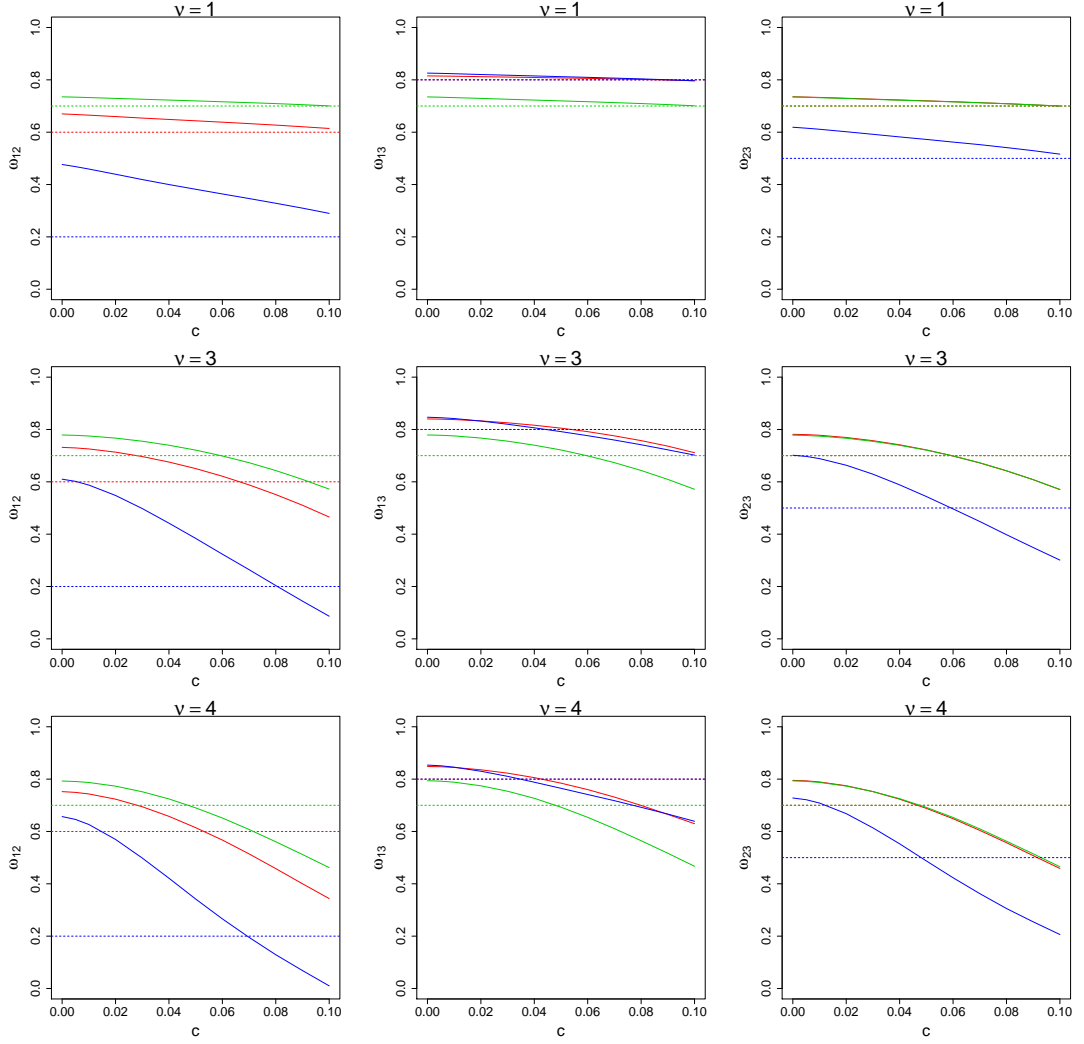


Figure 6: Mean approximate likelihood estimates for the trivariate ($d = 3$) extremal- t dependence parameters $\omega = (\omega_{1,2}, \omega_{1,3}, \omega_{2,3})^\top$ as a function of the threshold $c \geq 0$, based on 1000 replicate datasets. Columns denote mean approximate likelihood estimates of ω_{12} (left), ω_{13} (middle) and ω_{23} (right), whereas rows indicate the (fixed) degree of freedom of $\nu = 1$ (top), 3 (middle) and 4 (bottom). In all panels solid lines correspond to the mean approximate likelihood estimate and dashed lines denote the true parameter value. Red, green and blue lines respectively indicate the dependence parameters $\omega = (0.6, 0.8, 0.7)^\top, (0.7, 0.7, 0.7)^\top$ and $(0.2, 0.8, 0.5)^\top$.

proximate likelihood are more variable and perhaps less accurate as n increases, although the differences are not substantial. While the pairwise composite likelihood is more accurate and precise, it requires substantially more computation in numbers of likelihood terms ($n(n - 1)/2$) compared to the approximate likelihood (n).

For our second study, we compare the efficiency of the maximum triplewise composite likelihood estimator with that based on the pairwise composite likelihood. We generate 300 replicate samples of size $n = 20, 50$ and 70 from the extremal- t process with correlation function (9) with varying parameters, over 20 random spatial points on $\mathbb{S} = [0, 100]^2$.

Table 2 presents the resulting relative efficiencies $RE_\xi/RE_\lambda/RE_{(\lambda, \xi)}$ ($\times 100$), where $RE_\xi = \widehat{\text{var}}(\hat{\xi}_3)/\widehat{\text{var}}(\hat{\xi}_2)$, $RE_\lambda = \widehat{\text{var}}(\hat{\lambda}_3)/\widehat{\text{var}}(\hat{\lambda}_2)$ and $RE_{(\lambda, \xi)} = \widehat{\text{cov}}(\hat{\lambda}_3, \hat{\xi}_3)/\widehat{\text{cov}}(\hat{\lambda}_2, \hat{\xi}_2)$, where $(\hat{\lambda}_p, \hat{\xi}_p)$ are

Method		ω_{12}	ω_{13}	ω_{23}
$n = 500$	Full	0.600(0.039)	0.800(0.019)	0.698(0.030)
	Pairwise	0.600(0.041)	0.800(0.019)	0.698(0.030)
	Approximate	0.621(0.056)	0.791(0.036)	0.696(0.048)
$n = 100$	Full	0.590(0.094)	0.797(0.045)	0.694(0.067)
	Pairwise	0.591(0.095)	0.798(0.045)	0.694(0.068)
	Approximate	0.605(0.133)	0.785(0.086)	0.681(0.117)
$n = 50$	Full	0.583(0.135)	0.792(0.066)	0.688(0.101)
	Pairwise	0.581(0.155)	0.792(0.066)	0.689(0.102)
	Approximate	0.595(0.186)	0.774(0.133)	0.679(0.161)
True		0.600	0.800	0.700

Table 1: Mean maximum likelihood estimates of the extremal- t dependence parameters, based on 1000 replicate datasets. Estimates are based on full, pairwise composite and approximate likelihoods and varying sample sizes $n = 50, 100$ and 500 , with standard errors reported in parentheses. The degrees of freedom are fixed at $\nu = 3$, and $c = 0.06$ for the approximate likelihood.

the p -wise maximum composite likelihood estimates ($p = 2, 3$), and $\widehat{\text{var}}$ and $\widehat{\text{cov}}$ denote sample variance and covariance over replicates.

Perhaps unsurprisingly, the triplewise estimates are at worst just as efficient as the pairwise estimates ($RE \leq 100$) but are frequently much more efficient. However this is balanced computationally as there is a corresponding increase in the number of components in the triplewise composite likelihood function. For each ν , there is a general gain in efficiency when the smoothing parameter ξ increases for each fixed scale parameter λ . There is a similar gain when increasing λ for fixed ξ . These gains become progressively pronounced with increasing sample size n , and when there is stronger dependence present (i.e. smaller degrees of freedom ν). However, we note that there are a number of instances where the efficiency gain goes against this general trend, which indicates that there are some subtleties involved.

5 Discussion

Appropriate modelling of extremal dependence is critical for producing realistic and precise estimates of future extreme events. In practice this is a hugely challenging task, as extremes in different application areas may exhibit different types of dependence structures, asymptotic dependence levels, exchangeability, and stationary or non-stationary behaviour.

Working with families of skew-normal distributions and processes we have derived flexible new classes of extremal dependence models. Their flexibility arises as they include a wide range of dependence structures, while also incorporating several previously developed and popular models, such as the stationary extremal- t process and its sub-processes. This includes dependence structures that are asymptotically independent, which is useful for describing the dependence of variables that are not exchangeable, and a wide class of non-stationary, asymptotically dependent models, suitable for the modelling of spatial extremes.

In terms of future development, semi-parametric estimation methods would provide powerful techniques to fully take advantage of the flexibility offered by non-stationary max-stable models. Such methods can be computationally demanding, however. An interesting further direction would be to design simple and interpretable families of covariance functions for skew-normal processes for which it is then possible to derive max-stable dependence models that are useful

in practical applications.

A Appendix A: Proofs

A.1 Proof of Proposition 1

Items (1)–(3) are easily derived following the proof of Propositions (1)–(4) of Arellano-Valle and Genton (2010) and taking into account the next result.

Lemma 1. *Let $Y = (Y_1^\top, Y_2^\top)^\top \sim \mathcal{T}_d(\mu, \Omega, \kappa, \nu)$, where $Y_1 \in \mathbb{R}$ and $Y_2 \in \mathbb{R}^{d-1}$ with the corresponding partition of the parameters (μ, Ω, ν) and $\kappa = (\kappa_1, 0^\top)^\top$ with $\kappa_1 \in \mathbb{R}$. Then,*

$$(Y_1 | Y_2 = y_2) \sim \mathcal{T}(\mu_{1.2}, \Omega_{11.2}, \kappa_{1.2}, \nu_{1.2}), \quad y_2 \in \mathbb{R}^{d-1}$$

where $\mu_{1.2} = \mu_1 + \Omega_{12}\Omega_{22}^{-1}(y_2 - \mu_2)$, $\Omega_{1.2} = \zeta_2\Omega_{11.2}$, $\zeta_2 = \{\nu + Q_{\Omega_{22}^{-1}}(z_2)\}/(\nu + d_2)$, $z_2 = \omega_2^{-1}(y_2 - \mu_2)/\Omega_2$, $\omega_2 = \text{diag}(\Omega_{22})^{1/2}$, $\Omega_{11.2} = \Omega_{11} - \Omega_{12}\Omega_{22}^{-1}\Omega_{21}$, $\kappa_{1.2} = \zeta_2^{-1/2}\kappa$, $\nu_{1.2} = \nu + d - 1$

Proof of Lemma 1. The marginal density of Y_2 is equal to

$$f_{Y_2}(y_2) = \int_0^\infty \frac{v^{\nu/2-1}e^{-v}}{\Gamma(\nu/2)} \phi_{d-1} \left(\frac{y_2 - \mu_2}{\sqrt{\frac{\nu}{2v}}}; \Omega_{22} \right) \left(\frac{2v}{\nu} \right)^{(d-1)/2} dv = \psi_{d-1}(y_2; \mu_2, \Omega_{22}, \nu),$$

namely it is a $(d-1)$ -dimensional central t pdf. The joint density of Y is equal to

$$\begin{aligned} & f_{Y_2}(y_2) f_{Y_1|Y_2=y_2}(y_1) \\ &= \psi_{d-1}(y_2; \mu_2, \Omega_{22}, \nu) \int_0^\infty \frac{v^{(\nu+d-1)/2-1}e^{-v}}{\Gamma(\frac{\nu+d-1}{2})} \phi \left\{ (\Omega_{1.2})^{-1/2}(y_1 - \mu_{1.2}) \sqrt{\frac{2v}{\nu+d-1}} - (\Omega_{11.2})^{-1/2}\kappa_1 \right\} dv \\ &= \int_0^\infty \frac{(\Omega_{11.2})^{-1/2}v^{\nu/2-1}e^{-v}}{\Gamma(\frac{\nu}{2})} \left(\frac{2v}{\nu} \right)^{d/2} \phi_{d-1} \left(\frac{y_2 - \mu_2}{\sqrt{\frac{\nu}{2v}}} \right) \phi \left\{ (\Omega_{11.2})^{1/2}(y_1 - \mu_{1.2}) \sqrt{\frac{2v}{\nu}} - \kappa_1 \right\} dv \\ &= \int_0^\infty \frac{v^{\nu/2-1}e^{-v}}{\Gamma(\frac{\nu}{2})} \phi_d \left\{ \begin{pmatrix} y_1 - \mu_1 - \kappa_1 \sqrt{\frac{\nu}{2v}} \\ y_2 - \mu_2 \end{pmatrix}; \sqrt{\frac{\nu}{2v}}\Omega \right\} dv \end{aligned}$$

□

A.2 Proof of Proposition 2

Let $Z_s(h) = Z(s+h) - Z(s)$, with $s, h \in \mathbb{R}$. From Azzalini (e.g. 2013, Ch. 5) it follows that $Z_s(h) \sim \mathcal{SN}(\omega_s^2(h), \alpha_s(h), \tau)$, where

$$\omega_s^2(h) = 2(1 - \delta(s+h)\delta(s) - \rho(h)[\{1 - \delta^2(s+h)\}\{1 - \delta^2(s)\}]^{1/2})$$

and

$$\alpha_s^2(h) = \frac{\delta(s+h) - \delta(s)}{\{2(1 - \{\delta(s+h) + \delta(s)\}/2 - \rho(h)[\{1 - \delta^2(s+h)\}\{1 - \delta^2(s)\}]^{1/2})\}^{1/2}}.$$

Therefore, it follows that $\text{Var}\{Z_s(h)\} = 2\{1 - r_s(h)\} \equiv \sigma_s^2(h)$, where

$$r_s(h) = r/2\{\delta(s+h) - \delta(s)\}^2 + \delta(s+h)\delta(s) + \rho(h)[\{1 - \delta^2(s+h)\}\{1 - \delta^2(s)\}]^{1/2}$$

and r is as in (8). By the assumption on $\delta(s)$ we have that $r_s(h) = \rho(h) + \delta^2(s)(1 - \rho(h)) + o(1)$, as $h \rightarrow 0$. Using this and the assumption on $\rho(h)$ we obtain $1 - r_s(h) = O(|\log |h||^{-a})$, as $h \rightarrow 0$. Now, if $Z \sim \mathcal{SN}(\alpha, \tau)$, then $\Pr(|Z| > z) \leq 2\{1 - \Phi(z; |\alpha|, \tau)\}$. Furthermore, for $\alpha > 0$ the tail behavior of the skew-normal distribution satisfies the condition

$$1 - \Phi(z; \alpha, \tau) \leq K^{-1}\{1 - \Phi(z)\}, \quad x > 0,$$

where $K = \Phi\{\tau/(1 + \alpha^2)^{1/2}\}$. Putting these two results together we obtain that for a non-decreasing function $g(h)$, the following inequality

$$\Pr\{|Z_s(h)| > g(h)\} \leq 2K^{-1}[1 - \Phi\{g(h)/\sigma_s(h)\}],$$

holds. Note that we obtained then the same inequality of Lindgren (2012, page 48) apart from the constant K . Therefore, the remaining part of the proof follows in the same way as the proof provided therein.

A.3 Proof of Proposition 3

Recall that if $Z \sim \mathcal{SN}_2(\bar{\Omega}, \alpha)$, then $Z_j \sim \mathcal{SN}(\alpha_j^*)$ and $Z_j | Z_{3-j} \sim \mathcal{SN}(\alpha_{j \cdot 3-j})$ for $j=1,2$ (e.g. Azzalini (2013, Ch. 2) or Proposition 1), where

$$\alpha_j^* = \frac{\alpha_j + \omega\alpha_{3-j}}{\sqrt{1 + \alpha_{3-j}^2(1 - \omega^2)}}, \quad \alpha_{j \cdot 3-j} = \alpha_j\sqrt{1 - \omega^2}.$$

Define $x_j(u) = \Phi^\leftarrow(1 - u; \alpha_j^*)$, for any $u \in [0, 1]$, where $\Phi^\leftarrow(\cdot; \alpha_j^*)$ is the inverse of the marginal distribution function $\Phi(\cdot; \alpha_j^*)$, $j = 1, 2$. The asymptotic behaviour of $x_j(u)$ as $u \rightarrow 0$ is

$$x_j(u) = \begin{cases} x(u), & \text{if } \alpha_j^* \geq 0 \\ x(u)/\bar{\alpha}_j - \{2\log(1/u)\}^{-1/2}\log(\sqrt{\pi}\alpha_j^*), & \text{if } \alpha_j^* < 0 \end{cases} \quad (23)$$

for $j = 1, 2$, where $\bar{\alpha}_j = \{1 + \alpha_j^{*2}\}^{1/2}$ and $x(u) \approx \{2\log(1/u)\}^{1/2} - \{2\log(1/u)\}^{-1/2}\{\log\log(1/u) + \log(2\sqrt{\pi})\}$ (Padoan, 2011). The limiting behaviour of the joint survivor function of the bivariate skew-normal distribution is described by

$$p(u) = \Pr\{Z_1 > x_1(u), Z_2 > x_2(u)\}, \quad u \rightarrow 0. \quad (24)$$

For case (a), when $\alpha_1, \alpha_2 > 0$, then $x_1(u) = x_2(u) = x(u)$, and the joint upper tail (24) behaves as

$$\begin{aligned} p(u) &= \int_{x(u)}^{\infty} \left\{ 1 - \Phi\left(\frac{y(u) - \omega v}{\sqrt{1 - \omega^2}}; \alpha_{1,2}\right) \right\} \phi(v; \alpha_2^*) dv \\ &\approx \frac{\sqrt{1 - \omega^2}}{x(u)} \int_0^{\infty} \frac{\phi_2(x(u), x(u) + t/x(u); \bar{\Omega}, \alpha)}{x(u)(1 - \omega) - \omega t/x(u)} dt \\ &\approx \frac{e^{-x^2(u)/(1+\omega)}}{\pi(1 - \omega)x^2(u)} \left(\int_0^{\infty} e^{-t/(1+\omega)} dt - \frac{e^{-x^2(u)(\alpha_1 + \alpha_2)^2/2}}{\sqrt{2\pi}(\alpha_1 + \alpha_2)x(u)} \int_0^{\infty} e^{-t\{1/(1+\omega) + \alpha_2(\alpha_1 + \alpha_2)\}} dt \right) \\ &= \frac{e^{-x^2(u)/(1+\omega)}(1 + \omega)}{\pi(1 - \omega)x(u)^2} \left(1 - \frac{e^{-x^2(u)(\alpha_1 + \alpha_2)^2/2}}{\sqrt{2\pi}(\alpha_1 + \alpha_2)\{1 + \alpha_2(\alpha_1 + \alpha_2)(1 + \omega)\}x(u)} \right), \end{aligned} \quad (25)$$

as $u \rightarrow 0$. The first approximation is obtained by using $1 - \Phi(x; \alpha) \approx \phi(x; \alpha)/x$ as $x \rightarrow +\infty$, when $\alpha > 0$ (Padoan, 2011). The second approximation uses $1 - \Phi(x) \approx \phi(x)/x$ as $x \rightarrow +\infty$

(Feller, 1968). Let $X_j = \{-1/\log \Phi(Z_j; \alpha_j^*)\}$, $j = 1, 2$. Substituting $x(u)$ into (25) substituting and using the approximation $1 - \Pr(X_j > x) \approx 1/x$ as $x \rightarrow \infty$, $j = 1, 2$, we obtain that (24) with common unit Fréchet margins behaves asymptotically as $\mathcal{L}(x) x^{-2/(1+\omega)}$, as $x \rightarrow +\infty$, where

$$\mathcal{L}(x) = \frac{2(1+\omega)(4\pi \log x)^{-\omega/(1+\omega)}}{1-\omega} \left(1 - \frac{(4\pi \log x)^{\{(\alpha_1+\alpha_2)^2-1\}/2} x^{-(\alpha_1+\alpha_2)^2}}{(\alpha_1+\alpha_2)\{1+\alpha_2(\alpha_1+\alpha_2)(1+\omega)\}} \right). \quad (26)$$

As the second term in the parentheses in (26) is $o(x^{(\alpha_1+\alpha_2)})$, then the quantity inside the parentheses $\rightarrow 1$ rapidly as $x \rightarrow \infty$, and so $\mathcal{L}(x)$ is well approximated by the first term in (26). When $\alpha_2 < 0$ and $\alpha_1 \geq -\alpha_2/\omega$, then $\alpha_1^*, \alpha_2^* > 0$ and we obtain the same outcome.

For case (b), when $\alpha_2 < 0$ and $-\omega, \alpha_2 \leq \alpha_1 < -\omega^{-1}\alpha_2$, then $\alpha_1^* \geq 0$ and $\alpha_2^* < 0$ and hence $x_1(u) = x(u)$ and $x_2(u) \approx x(u)/\bar{\alpha}_2$ as $u \rightarrow 0$. When $\alpha_1 > -\bar{\alpha}_2\alpha_2$, then following a similar derivation to those in (25), we obtain that

$$p(u) \approx \frac{\bar{\alpha}_2^2(1-\omega^2)(1-\omega\bar{\alpha}_2)^{-1}}{\pi(\bar{\alpha}_2-\omega)x^2(u)} \exp \left[-\frac{x^2(u)}{2} \left\{ \frac{1-\omega^2+(\bar{\alpha}_2-\omega)^2}{(1-\omega^2)\bar{\alpha}_2^2} \right\} \right], \quad \text{as } u \rightarrow 0.$$

Similarly, when $\alpha_1 < -\bar{\alpha}_2\alpha_2$, and noting that $\Phi(x) \approx -\phi(-x)/x$ as $x \rightarrow -\infty$, then

$$p(u) \approx \frac{-\bar{\alpha}_2^2\{1-\omega\bar{\alpha}_2+\alpha_2(\alpha_2+\alpha_1\bar{\alpha}_2)(1-\omega^2)\}^{-1}}{\pi(\bar{\alpha}_2-\omega)(1-\omega^2)^{-1}(\alpha_1+\alpha_2/\bar{\alpha}_2)x^3(u)} e^{-\frac{x^2(u)}{2} \left\{ \frac{1-\omega^2+(\bar{\alpha}_2-\omega)^2}{(1-\omega^2)\bar{\alpha}_2^2} + \left(\alpha_1 + \frac{\alpha_2}{\bar{\alpha}_2} \right)^2 \right\}}, \quad \text{as } u \rightarrow 0.$$

For case (c), when $\alpha_2 < 0$ and $0 < \alpha_1 < -\omega\alpha_2$, then $\alpha_1^*, \alpha_2^* < 0$ and hence $x_1(u) \approx x(u)/\bar{\alpha}_1$ and $x_2(u) \approx x(u)/\bar{\alpha}_2$ as $u \rightarrow 0$. Then as $u \rightarrow 0$ we have

$$p(u) \approx \frac{-\bar{\alpha}_2^{3/2}\bar{\alpha}_1^2(1-\omega^2)(\bar{\alpha}_2-\omega\bar{\alpha}_1)^{-1}(\alpha_1\bar{\alpha}_2+\alpha_2\bar{\alpha}_1)^{-1}}{\pi\{1-\omega\bar{\alpha}_2+\alpha_2(\alpha_2+\alpha_1\bar{\alpha}_2/\bar{\alpha}_1)(1-\omega^2)\}x^3(u)} \times \exp \left[-\frac{x^2(u)}{2(1-\omega^2)} \left(\frac{\alpha_1^2(1-\omega^2)+1}{\bar{\alpha}_1^2} + \frac{\alpha_2^2(1-\omega^2)+1}{\bar{\alpha}_2^2} + \frac{2(\alpha_1\alpha_2(1-\omega^2)-\omega)}{\bar{\alpha}_1\bar{\alpha}_2} \right) \right] \quad u \rightarrow 0.$$

When $\alpha_1, \alpha_2 < 0$ and $\omega_2^{-1}\alpha_2 \leq \alpha_1 < 0$ the same argument holds. Finally, interchanging α_1 with α_2 produces the same results but substituting α_j and $\bar{\alpha}_j$ with α_{3-j} and $\bar{\alpha}_{3-j}$ respectively, for $j = 1, 2$.

A.4 Proof of Proposition 4

Let $Z \sim \mathcal{ST}(\alpha, \tau, \kappa, \nu)$. Then $1 - \Psi(x; \alpha, \tau, \nu) \approx x^{-\nu} \mathcal{L}(x; \alpha, \tau, \nu)$ as $x \rightarrow +\infty$, for any $\nu > 1$, where

$$\mathcal{L}(x; \alpha, \tau, \kappa, \nu) = \frac{\Gamma\{(\nu+1)/2\}\Psi(\alpha\sqrt{\nu+1}; \nu+1)}{\Gamma(\nu/2)\sqrt{\pi}\nu^{3/2}\Psi(\tau/\sqrt{1+\alpha^2}; \kappa/\sqrt{1+\alpha^2}, \nu)} \left(\frac{1}{x^2} + \frac{1}{\nu} \right)^{-(\nu+1)/2}$$

is a slowly varying function (e.g de Haan and Ferreira, 2006, Appendix B). From Corollary 1.2.4 in de Haan and Ferreira (2006), it follows that the normalisation constants are $a_n = \Psi^\leftarrow(1 - 1/n; \alpha, \tau, \kappa, \nu)$, where Ψ^\leftarrow is the inverse function of Ψ , and $b_n = 0$, and therefore $a_n = \{n\mathcal{L}(\alpha, \tau, \kappa, \nu)\}^{1/\nu}$, where $\mathcal{L}(\alpha, \tau, \kappa, \nu) \equiv \mathcal{L}(\infty; \alpha, \tau, \kappa, \nu)$. Applying Theorem 1.2.1 in de Haan and Ferreira (2006) we obtain that $M_n/a_n \Rightarrow U$, where U has ν -Fréchet univariate marginal distributions.

Let $Z \sim \mathcal{ST}_d(\bar{\Omega}, \alpha, \tau, \kappa, \nu)$. For any $j \in \{1, \dots, d\}$ consider the partition $Z = (Z_j, Z_{I_j}^\top)^\top$, where $I_j = \{1, \dots, d\} \setminus j$ and $Z_j = Z_{\{j\}}$, and the respective partition of $(\bar{\Omega}, \alpha)$. Define $a_n =$

$(a_{n,1}, \dots, a_{n,d})$, where $a_{n,j} = \{n\mathcal{L}(\alpha_j^*, \tau_j^*, \kappa_j^*, \nu)\}^{1/\nu}$ and $\alpha_j^* = \alpha_{\{j\}}^*$, $\tau_j^* = \tau_{\{j\}}^*$ and $\kappa_j^* = \kappa_{\{j\}}^*$ are the marginal parameters (5) under Proposition 1(1). From Theorem 6.1.1 and Corollary 6.1.3 in de Haan and Ferreira (2006), $M_n/a_n \Rightarrow U$, where the distribution of U is $G(x) = \exp\{-V(x)\}$ with $V(x) = \lim_{n \rightarrow +\infty} n\{1 - \Pr(Z_1 \leq a_{n,1}x_1, \dots, Z_d \leq a_{n,d}x_d)\}$ for all $x = (x_1, \dots, x_d)^\top \in \mathbb{R}_+^d$. Applying the conditional tail dependence function framework of Nikoloulopoulos et al. (2009) it follows that

$$V(x_j, i \in I) = \lim_{n \rightarrow \infty} \sum_{j=1}^d x_j^{-\nu} \Pr(Z_i \leq a_{n,i}x_i, i \in I_j | Z_j = a_{n,j}x_j).$$

From the conditional distribution in Proposition 1(1) we have that

$$\left\{ \left(\frac{Z_i - a_{n,j}x_j}{\{\zeta_{n,j}(1 - \omega_{i,j}^2)\}^{1/2}}, i \in I_j \right)^\top | Z_j = a_{n,j}x_j \right\} \sim \mathcal{ST}_{d-1} \left(\bar{\Omega}_j^+, \alpha_j^+, \tau_{n,j}, \kappa_{n,j}, \nu + 1 \right),$$

for $j \in \dots, 1, \dots, d$, where $\bar{\Omega}_j^+ = \omega_{I_j I_j \cdot j}^{-1} \Omega_{I_j I_j \cdot j} \omega_{I_j I_j \cdot j}^{-1}$, $\omega_{I_j I_j \cdot j} = \text{diag}(\Omega_{I_j I_j \cdot j})^{1/2}$, $\bar{\Omega}_{I_j I_j \cdot j} = \bar{\Omega}_{I_j I_j} - \bar{\Omega}_{I_j j} \bar{\Omega}_{j I_j}$, $\alpha_j^+ = \bar{\Omega}_{I_j I_j \cdot j} \alpha_{I_j}$, $\zeta_{n,j} = [\nu + (a_{n,j}x_j)^2]/(\nu + 1)$, $\tau_{n,j} = [(\bar{\Omega}_{j I_j} \alpha_{I_j} + \alpha_j)a_{n,j}x_j + \tau]/\zeta_{n,j}^{1/2}$ and $\kappa_{n,j} = \kappa/\zeta_{n,j}^{1/2}$. Now, for any $j \in \{1, \dots, d\}$ and all $i \in I_j$

$$\frac{a_{n,i}x_i - a_{n,j}x_j}{\{\zeta_{n,j}(1 - \omega_{i,j}^2)\}^{1/2}} \rightarrow \frac{(x_i^*/x_j^* - \omega_{i,j})(\nu + 1)^{1/2}}{\{(1 - \omega_{i,j})\}^{1/2}} \quad \text{as } n \rightarrow +\infty,$$

where $\omega_{i,j}$ is the (i, j) -th element of $\bar{\Omega}$, $x_j^+ = x_j \mathcal{L}^{1/\nu}(\alpha_j^*, \tau_j^*, \kappa_j^*, \nu)$ and $\tau_{n,j} \rightarrow \tau_j^+ = (\bar{\Omega}_{j I_j} \alpha_{I_j} + \alpha_j)(\nu + 1)^{1/2}$, and $\kappa_{n,j} \rightarrow 0$ as $n \rightarrow +\infty$. As a consequence

$$V(x_j, j \in I) = \sum_{j=1}^d x_j^{-\nu} \Psi_{d-1} \left(\left(\sqrt{\frac{\nu + 1}{1 - \omega_{i,j}^2}} \left(\frac{x_i^+}{x_j^+} - \omega_{i,j} \right), i \in I_j \right)^\top; \bar{\Omega}_j^+, \alpha_j^+, \tau_j^+, \nu + 1 \right).$$

A.5 Proof of Theorem 1

Let $Y(s)$ be a skew-normal process with finite dimensional distribution $\mathcal{SN}_d(\bar{\Omega}, \alpha, \tau)$. For any $j \in I = \{1, \dots, d\}$ consider the partition $Y = (Y_j, Y_{I_j}^\top)^\top$, where $I_j = I \setminus j$, $Y_j = Y_{\{j\}} = Y(s_j)$ and $Y_{I_j} = (Y_i, i \in I_j)^\top$, and the respective partition of $(\bar{\Omega}, \alpha)$. The exponent function (14) is

$$V(x_j, j \in I) = \mathbb{E} \left[\max_j \left\{ \frac{(Y_j^+ / x_j)^\xi}{m_j^+} \right\} \right] = \int_{\mathbb{R}^d} \max_j \left\{ \frac{(y_j / x_j)^\xi}{m_j^+}, 0 \right\} \phi_d(y; \bar{\Omega}; \alpha, \tau) dy,$$

where $x_j \equiv x(s_j)$, $y_j \equiv y(s_j)$ and $m_j^+ \equiv m^+(s_j)$. Then

$$V(x_j, j \in I) = \sum_{j=1}^d V_j, \quad V_j = \frac{1}{m_j^+} \int_0^\infty \left(\frac{y_j}{x_j} \right)^\nu \int_{-\infty}^{y_j x_{I_j} / x_j} \phi_d(y; \bar{\Omega}; \alpha, \tau) dy_{I_j} dy_j, \quad (27)$$

where $x_{I_j} = (x_i, i \in I_j)^\top$ and $y_{I_j} = (y_i, i \in I_j)^\top$. As $Y_j \sim \mathcal{SN}(\alpha_j^*, \tau_j^*)$, where $\alpha_j^* = \alpha_{\{j\}}^*$ and $\tau_j^* = \tau_{\{j\}}^*$ are the marginal parameters derived from Proposition 1(1), then

$$\begin{aligned} m_j^+ &= \int_0^\infty y_j^\nu \phi(y_j; \alpha_j^*, \tau_j^*) dy_j = \frac{1}{\Phi\{\tau_j^*(1 + \alpha_j^{*2})^{-1/2}\}} \int_0^\infty y_j^\nu \phi(y_j) \Phi(\alpha_j^* y_j + \tau_j^*) dy_j \\ &= \frac{2^{(\nu-2)/2} \Gamma\{(\nu+1)/2\} \Psi(\alpha_j^* \sqrt{\nu+1}; -\tau_j^*, \nu+1)}{\sqrt{\pi} \Phi[\tau\{1 + Q_{\bar{\Omega}}(\alpha)\}^{-1/2}]} \end{aligned}$$

by observing that $\tau_j^* \{1 + \alpha_j^{*2}\}^{1/2} = \tau \{1 + Q_{\bar{\Omega}}(\alpha)\}^{-1/2}$.

For $j = 1, \dots, d$ define $x_j^\circ = x_j(m_j^+)^{1/\nu}$ and $m_j^+ = \bar{m}_j^+ / \Phi[\tau \{1 + Q_{\bar{\Omega}}(\alpha)\}^{-1/2}]$, where $\bar{m}_j^+ = (\pi)^{1/2} 2^{(\nu-2)/2} \Gamma\{(\nu+1)/2\} \Psi(\alpha_j^* \sqrt{\nu+1}; -\tau_j^*, \nu+1)$. Then, for any $j = 1, \dots, d$

$$\begin{aligned} V_j &= \frac{1}{m_j^+} \int_0^\infty \left(\frac{y_j}{x_j} \right)^\nu \int_{-\infty}^{y_j x_{I_j} / x_j} \phi_d(y; \bar{\Omega}, \alpha, \tau) dy_{I_j} dy_j \\ &= \frac{1}{\bar{m}_j^+} \int_0^\infty \left(\frac{y_j}{x_j} \right)^\nu \int_{-\infty}^{y_j x_{I_j} / x_j} \phi_d(y; \Omega) \Phi(\alpha^\top y + \tau) dy_{I_j} dy_j \\ &= \frac{1}{\bar{m}_j^+} \int_0^\infty \left(\frac{y_j}{x_j} \right)^\nu \phi(y_j) \int_{-\infty}^{y_j x_{I_j} / x_j} \phi_{d-1}(y_{I_j} - y_j \bar{\Omega}_{j,I_j}; \bar{\Omega}_j^\circ) \Phi(\alpha^\top y + \tau) dy_{I_j} dy_j \\ &= \frac{1}{\bar{m}_j^+} \int_0^\infty \left(\frac{y_j}{x_j} \right)^\nu \phi(y_j) \Phi_d(y_j^\circ; \Omega_j^\circ) dy_j, \end{aligned}$$

where

$$y_j^\circ = \begin{pmatrix} y_j \omega_{I_j I_j \cdot j}^{-1} (x_{I_j}^\circ / x_j^\circ - \bar{\Omega}_{I_j j}) \\ y_j \alpha_j^* + \tau_j^* \end{pmatrix},$$

with $\omega_{I_j I_j \cdot j} = \text{diag}(\bar{\Omega}_{I_j I_j \cdot j})^{1/2}$, $\bar{\Omega}_{I_j I_j \cdot j} = \bar{\Omega}_{I_j I_j} - \bar{\Omega}_{I_j j} \bar{\Omega}_{j I_j}$, $y_j \alpha_j^* + \tau_j^* = \frac{y_j (\alpha_j + \bar{\Omega}_{j j}^{-1} \bar{\Omega}_{j I_j} \alpha_{I_j}) + \tau}{\{1 + Q_{\bar{\Omega}_{I_j I_j \cdot j}}(\alpha_{I_j})\}^{1/2}}$ and

$$\Omega_j^{\circ\circ} = \begin{pmatrix} \bar{\Omega}_j^\circ & -\frac{\bar{\Omega}_{I_j I_j \cdot j} \omega_{I_j I_j \cdot j}^{-1} \alpha_{I_j}}{\{1 + Q_{\bar{\Omega}_{I_j I_j \cdot j}}(\alpha_{I_j})\}^{1/2}} \\ -\left(\frac{\bar{\Omega}_{I_j I_j \cdot j} \omega_{I_j I_j \cdot j}^{-1} \alpha_{I_j}}{\{1 + Q_{\bar{\Omega}_{I_j I_j \cdot j}}(\alpha_{I_j})\}^{1/2}} \right)^\top & 1 \end{pmatrix},$$

where $\bar{\Omega}_j^\circ = \omega_{I_j I_j \cdot j}^{-1} \bar{\Omega}_{I_j I_j \cdot j} \omega_{I_j I_j \cdot j}^{-1}$ and $\frac{\Omega_{I_j I_j \cdot j} \omega_{I_j I_j \cdot j}^{-1} \alpha_{I_j}}{\{1 + Q_{\bar{\Omega}_{I_j I_j \cdot j}}(\alpha_{I_j})\}^{1/2}} = \frac{\Omega_j^\circ \omega_{I_j I_j \cdot j} \alpha_{I_j}}{\{1 + Q_{\bar{\Omega}_j^\circ}(\omega_{I_j I_j \cdot j} \alpha_{I_j})\}^{1/2}}$.

Applying Dutt's (Dutt, 1973) probability integrals we obtain

$$\begin{aligned} V_j &= \frac{1}{\bar{m}_j^+} \int_0^\infty \left(\frac{y_j}{x_j} \right)^\nu \phi(y_j) \Phi_d(y_j^\circ; \Omega_j^\circ) dy_j, \\ &= \frac{1}{x_j^\nu} \frac{\Psi_{d+1} \left(\left(\left(\sqrt{\frac{\nu+1}{1-\omega_{i,j}^2}} \left(\frac{x_i^\circ}{x_j^\circ} - \omega_{i,j} \right), i \in I_j \right), \alpha_j^* \sqrt{\nu+1} \right)^\top; \Omega_j^{\circ\circ}, (0, -\tau_j^*)^\top, \nu+1 \right)}{\Psi(\alpha_j^* \sqrt{\nu+1}; -\tau_j^*, \nu+1)}. \end{aligned}$$

This is recognised as the form of a $(d-1)$ -dimensional non-central extended skew- t distribution with $\nu+1$ degrees of freedom (Jamalizadeh et al., 2009), from which V_j can be expressed as

$$V_j = \frac{1}{x_j^\nu} \Psi_{d-1} \left(\left(\sqrt{\frac{\nu+1}{1-\omega_{i,j}^2}} \left(\frac{x_i^\circ}{x_j^\circ} - \omega_{i,j} \right), i \in I_j \right)^\top; \bar{\Omega}_j^\circ, \alpha_j^\circ, \tau_j^\circ, \kappa_j^\circ, \nu+1 \right)$$

for $j = 1, \dots, d$ where $\alpha_j^\circ = \omega_{I_j I_j \cdot j} \alpha_{I_j}$, $\tau_j^\circ = (\bar{\Omega}_{j I_j} \alpha_{I_j} + \alpha_j)(\nu+1)^{1/2}$ and $\kappa_j^\circ = -\{1 + Q_{\bar{\Omega}_{I_j I_j \cdot j}}(\alpha_{I_j})\}^{-1/2} \tau$. Substituting the expression for V_j into (27) then gives the required the exponent function.

B Appendix B: Computational details

B.1 Computation of d -dimensional extremal-skew- t density for $d = 2, 3, 4$.

For clarity of exposition we focus on the finite dimensional distribution G of the extremal- t process. We initially assume that $\alpha = 0$ and $\tau = 0$, and relax this assumption later. For brevity the exponent function is written as

$$V(x_j, j \in I) = \sum_{j \in I} x_j^{-1} T_j, \quad T_j = \Psi_{d-1}(u_j; \bar{\Omega}_j^\circ, \nu + 1)$$

where $I = \{1, \dots, d\}$, $u_j = \left[\sqrt{\frac{\nu+1}{1-\omega_{i,j}^2}} \left\{ \left(\frac{x_i}{x_j} \right)^{1/\nu} - \omega_{i,j} \right\}, i \in I_j \right]^\top$ and where $I_j = I \setminus \{j\}$. By successive differentiations the 2-dimensional density ($d = 2$) is

$$f(x) = (-V_{12} + V_1 V_2)G(x), \quad x \in \mathbb{R}_+^2,$$

the 3-dimensional density ($d = 3$) is

$$f(x) = (-V_{123} + V_1 V_{23} + V_2 V_{13} + V_3 V_{12} - V_1 V_2 V_3)G(x), \quad x \in \mathbb{R}_+^3$$

and the 4-dimensional density ($d = 4$) is

$$\begin{aligned} f(x) = & (-V_{1234} + V_1 V_{234} + V_2 V_{134} + V_3 V_{124} + V_{12} V_{34} + V_{13} V_{24} + V_{14} V_{23} \\ & - V_1 V_2 V_{34} - V_1 V_3 V_{24} - V_1 V_4 V_{23} - V_2 V_3 V_{14} - V_2 V_4 V_{13} - V_3 V_4 V_{12} \\ & + V_1 V_2 V_3 V_4)G(x), \quad x \in \mathbb{R}_+^4 \end{aligned}$$

where $V_{i_1, \dots, i_m} := \frac{d^m V(x_j, j \in I)}{dx_{i_1} \cdots dx_{i_m}}$ for $i_k \in I$. The derivatives of the exponent function are given by

$$V_{i_1, \dots, i_m} = \sum_{k=1}^d x_{i_k}^{-1} \frac{d^m T_{i_k}}{dx_{i_1} \cdots dx_{i_m}} - \sum_{\ell=1}^m x_{i_\ell}^{-2} \frac{d^{m-1} T_{i_\ell}}{dx_{i_1} \cdots dx_{i_{\ell-1}} dx_{i_{\ell+1}} \cdots dx_{i_m}}. \quad (28)$$

In particular, when $m = d$ it follows that $\{i_1, \dots, i_d\} = \{1, \dots, d\}$ and that

$$V_{1 \dots d} = -(\nu x_1)^{-(d+1)} \psi_{d-1}(u_1; \bar{\Omega}_1^\circ, \nu + 1) \prod_{i=2}^d \sqrt{\frac{\nu+1}{1-\omega_{i,1}^2}} \left(\frac{x_i}{x_1} \right)^{\frac{1}{\nu}-1}.$$

When $d = 2$ or 3 , the derivatives of T_j , for $j \in I$ are given by

$$\frac{dT_j}{dx_{i_1}} = \sum_{p=1}^{d-1} \frac{d}{du_{p,j}} \Psi_{d-1}(u_j; \bar{\Omega}_j^\circ, \nu + 1) \frac{du_{p,j}}{dx_{i_1}}, \quad (29)$$

$$\begin{aligned} \frac{d^2 T_j}{dx_{i_1} dx_{i_2}} = & \sum_{p=1}^{d-1} \left(\frac{d}{du_{p,j}} \Psi_{d-1}(u_j; \bar{\Omega}_j^\circ, \nu + 1) \frac{d^2 u_{p,j}}{dx_{i_1} dx_{i_2}} + \frac{d^2}{du_{p,j}^2} \Psi_{d-1}(u_j; \bar{\Omega}_j^\circ, \nu + 1) \frac{du_{p,j}}{dx_{i_1}} \frac{du_{p,j}}{dx_{i_2}} \right) \\ & + \sum_{p=1}^{d-2} \sum_{q=p+1}^{d-1} \frac{d^2}{du_{p,j} du_{q,j}} \Psi_{d-1}(u_j; \bar{\Omega}_j^\circ, \nu + 1) \left[\frac{du_{p,j}}{dx_{i_1}} \frac{du_{q,j}}{dx_{i_2}} + \frac{du_{p,j}}{dx_{i_2}} \frac{du_{q,j}}{dx_{i_1}} \right]. \end{aligned} \quad (30)$$

where $u_{p,j}$ is the p -th element of u_j , and when $d = 3$

$$\begin{aligned}
\frac{d^3 T_j}{dx_{i_1} dx_{i_2} dx_{i_3}} &= \sum_{p=1}^2 \sum_{q=2}^3 \left(\frac{d^2}{du_{p,j} du_{q,j}} \Psi_{d-1} (u_j; \bar{\Omega}_j^\circ, \nu + 1) \sum_{\substack{r,s,t \in I \\ r \neq s \neq t}} \frac{du_{p,j}}{dx_{i_r}} \frac{d^2 u_{q,j}}{dx_{i_s} dx_{i_t}} + \frac{du_{q,j}}{dx_{i_r}} \frac{d^2 u_{p,j}}{dx_{i_s} dx_{i_t}} \right) \\
&+ \sum_{p=1}^3 \sum_{\substack{q=1 \\ q \neq p}}^3 \frac{d^3}{du_{p,j}^2 du_{q,j}} \Psi_{d-1} (u_j; \bar{\Omega}_j^\circ, \nu + 1) \sum_{\substack{r,s,t \in I \\ r \neq s \neq t}} \frac{du_{p,j}}{dx_{i_r}} \frac{du_{p,j}}{dx_{i_s}} \frac{du_{q,j}}{dx_{i_t}} \\
&+ \frac{d^3}{du_{1,j} du_{2,j} du_{3,j}} \Psi_{d-1} (u_j; \bar{\Omega}_j^\circ, \nu + 1) \sum_{\substack{r,s,t \in I \\ r \neq s \neq t}} \frac{du_{1,j}}{dx_{i_r}} \frac{du_{2,j}}{dx_{i_s}} \frac{du_{3,j}}{dx_{i_t}}. \tag{31}
\end{aligned}$$

We provide the derivatives of the d -dimensional t cdf below. When $d = 1$ and for all $x \in \mathbb{R}_+$

$$\begin{aligned}
\frac{d}{dx} \Psi(x; \nu) &= \psi(x; \nu), \quad \frac{d^2}{dx^2} \Psi(x; \nu) = -\frac{(\nu + 1)x}{\nu + x^2} \psi(x; \nu), \\
\frac{d^3}{dx^3} \Psi(x; \nu) &= \frac{(\nu + 1)(x^2 - \nu + (\nu + 1)x^2)}{(\nu + x^2)^2} \psi(x; \nu).
\end{aligned}$$

When $d=2$ and for all $x \in \mathbb{R}_+^2$,

$$\begin{aligned}
\frac{d}{dx_1} \Psi_2(x; \bar{\Omega}, \nu) &= \psi(x_1; \nu) \Psi(v_{2,1}; \nu + 1), \\
\frac{d^2}{dx_1^2} \Psi_2(x; \bar{\Omega}, \nu) &= -\psi(x_1; \nu) \left\{ \frac{(\nu + 1)x_1}{\nu + x_1^2} \Psi(v_{2,1}; \nu + 1) + \sqrt{\frac{\nu + 1}{1 - \omega^2}} \left(\frac{\omega\nu + x_2 x_1}{(\nu + x_1^2)^{3/2}} \right) \psi(v_{2,1}; \nu + 1) \right\}, \\
\frac{d^2}{dx_1 dx_2} \Psi_2(x; \bar{\Omega}, \nu) &= \psi_2(x; \bar{\Omega}, \nu),
\end{aligned}$$

where $v_{i,j} = \sqrt{\frac{\nu+1}{\nu+x_j^2}} \frac{x_i - \omega_{i,j} x_1}{\sqrt{1-\omega_{i,j}^2}}$, $j \in I, j \in I_j$,

$$\begin{aligned}
\frac{d^3}{dx_1^3} \Psi_2(x; \bar{\Omega}, \nu) &= \Psi(v_{2,1}; \nu + 1) \psi(x_1; \nu) \left\{ \frac{(\nu + 1)^2 x_1^2 - (\nu + 1)(\nu - x_1^2)}{(\nu + x_1^2)^2} \right\} \\
&+ \psi(v_{2,1}; \nu + 1) \psi(x_1; \nu) \sqrt{\frac{\nu + 1}{1 - \omega^2}} \frac{1}{(\nu + x_1^2)^{5/2}} \\
&\times \left\{ x_1(\omega\nu + x_2 x_1)(2\nu - 1) - x_2(\nu + x_1^2) \right. \\
&\left. - \frac{(\omega(\nu + x_1^2) + (x_2 - \omega x_1)x_1)(\nu + 2)(x_2 - \omega x_1)(\omega\nu + x_2 x_1)}{(\nu + x_1^2)(1 - \omega^2) + (x_2 - \omega x_1)^2} \right\},
\end{aligned}$$

$$\frac{d^3}{dx_1^2 dx_2} \Psi_2(x; \bar{\Omega}, \nu) = -\frac{(\nu + 2)(x_1 - \omega x_2)}{2\pi\nu(1 - \omega^2)^{3/2}} \left(1 + \frac{x_1^2 - 2\omega x_1 x_2 + x_2^2}{\nu(1 - \omega^2)} \right)^{-(\frac{\nu}{2} + 1)}.$$

When $d=3$ and for all $x \in \mathbb{R}_+^3$,

$$\frac{d}{dx_1} \Psi_3(x; \bar{\Omega}, \nu) = \psi(x; \nu) \Psi_2 \left\{ (v_{2,1}, v_{3,1})^\top; \bar{\Omega}_1^\circ, \nu + 1 \right\},$$

$$\begin{aligned}
\frac{d^2}{dx_1^2} \Psi_3(x; \bar{\Omega}, \nu) &= \frac{-\psi(x_1; \nu)}{\nu + x_1^2} \left[(\nu + 1)x_1 \times \Psi_2 \left\{ (v_{2.1}, v_{3.1})^\top; \bar{\Omega}_1^\circ, \nu + 1 \right\} \right. \\
&+ \psi(v_{2.1}; \nu + 1) \sqrt{\frac{\nu + 1}{1 - \omega_{12}^2}} \frac{x_2 x_1 + \omega_{12} \nu}{\sqrt{\nu + x_1^2}} \\
&\times \Psi \left(\frac{\sqrt{\nu + 2} \left\{ (x_3 - \omega_{13} x_1)(1 - \omega_{12}^2) - (\omega_{23} - \omega_{12} \omega_{13})(x_2 - \omega_{12} x_1) \right\}}{\sqrt{\left\{ (1 - \omega_{12}^2)(\nu + x_1^2) + (x_2 - \omega_{12} x_1)^2 \right\} \left\{ (1 - \omega_{12}^2)(1 - \omega_{13}^2) - (\omega_{23} - \omega_{12} \omega_{13})^2 \right\}}; \nu + 2 \right) \\
&+ \psi(v_{3.1}; \nu + 1) \sqrt{\frac{\nu + 1}{1 - \omega_{13}^2}} \frac{x_3 x_1 + \omega_{13} \nu}{\sqrt{\nu + x_1^2}} \\
&\times \Psi \left(\frac{\sqrt{\nu + 2} \left\{ (x_2 - \omega_{12} x_1)(1 - \omega_{13}^2) - (\omega_{23} - \omega_{12} \omega_{13})(x_3 - \omega_{13} x_1) \right\}}{\sqrt{\left\{ (1 - \omega_{13}^2)(\nu + x_1^2) + (x_3 - \omega_{13} x_1)^2 \right\} \left\{ (1 - \omega_{12}^2)(1 - \omega_{13}^2) - (\omega_{23} - \omega_{12} \omega_{13})^2 \right\}}; \nu + 2 \right) \left. \right]
\end{aligned}$$

$$\begin{aligned}
\frac{d^2}{dx_1 dx_2} \Psi_3(x; \bar{\Omega}, \nu) &= \psi(x_2; \nu) \psi(v_{1.2}; \nu + 1) \sqrt{\frac{\nu + 1}{(1 - \omega_{12}^2)(\nu + x_2^2)}} \\
&\times \Psi \left(\frac{\sqrt{\nu + 2} \left\{ (x_3 - \omega_{23} x_2)(1 - \omega_{12}^2) - (\omega_{13} - \omega_{12} \omega_{23})(x_1 - \omega_{12} x_2) \right\}}{\sqrt{\left\{ (1 - \omega_{12}^2)(\nu + x_1^2) + (x_1 - \omega_{12} x_2)^2 \right\} \left\{ (1 - \omega_{12}^2)(1 - \omega_{23}^2) - (\omega_{13} - \omega_{12} \omega_{23})^2 \right\}}; \nu + 2 \right)
\end{aligned}$$

$$\begin{aligned}
\frac{d^3}{dx_1^2 dx_2} \Psi_3(x; \bar{\Omega}, \nu) &= -\psi(x_3; \nu) \psi(v_{1.3}; \nu + 1) \sqrt{\frac{\nu + 1}{(1 - \omega_{13}^2)(\nu + x_3^2)}} \left[\frac{(\nu + 2)(x_1 - \omega_{12} x_2)}{(1 - \omega_{12}^2)(\nu + x_2^2) + (x_1 - \omega_{12} x_2)^2} \right. \\
&\times \Psi \left(\frac{\sqrt{\nu + 2} \left\{ (x_3 - \omega_{23} x_2)(1 - \omega_{12}^2) - (\omega_{13} - \omega_{12} \omega_{23})(x_1 - \omega_{12} x_2) \right\}}{\sqrt{\left\{ (1 - \omega_{12}^2)(\nu + x_1^2) + (x_1 - \omega_{12} x_2)^2 \right\} \left\{ (1 - \omega_{12}^2)(1 - \omega_{23}^2) - (\omega_{13} - \omega_{12} \omega_{23})^2 \right\}}; \nu + 2 \right) \\
&+ \frac{\sqrt{\nu + 2}(1 - \omega_{12}^2)}{\sqrt{(1 - \omega_{12}^2)(1 - \omega_{23}^2) - (\omega_{13} - \omega_{12} \omega_{23})^2}} \frac{(\omega_{13} - \omega_{12} \omega_{23}) - (x_1 - \omega_{12} x_2)(x_3 - \omega_{23} x_2)}{\left\{ (1 - \omega_{12}^2)(\nu + x_2^2) + (x_1 - \omega_{12} x_2)^2 \right\}^{3/2}} \\
&\times \psi \left(\frac{\sqrt{\nu + 2} \left\{ (x_3 - \omega_{23} x_2)(1 - \omega_{12}^2) - (\omega_{13} - \omega_{12} \omega_{23})(x_1 - \omega_{12} x_2) \right\}}{\sqrt{\left\{ (1 - \omega_{12}^2)(\nu + x_1^2) + (x_1 - \omega_{12} x_2)^2 \right\} \left\{ (1 - \omega_{12}^2)(1 - \omega_{23}^2) - (\omega_{13} - \omega_{12} \omega_{23})^2 \right\}}; \nu + 2 \right) \left. \right]
\end{aligned}$$

$$\begin{aligned}
\frac{d^3}{dx_1^3} \Psi_3(x; \bar{\Omega}, \nu) = & -\frac{\psi(x_1; \nu)}{(\nu + x_1^2)} \left[\left(\frac{\nu + 3}{\nu + x_1^2} \right) (1 - x_1^2)(\nu + 1) \Psi_2 \left\{ (v_{2 \cdot 1}, v_{3 \cdot 1})^\top; \bar{\Omega}_1^\circ, \nu + 1 \right\} \right. \\
& + \Psi \left(\frac{\sqrt{\nu + 2} [(x_3 - \omega_{13}x_1)(1 - \omega_{12}^2) - (\omega_{23} - \omega_{12}\omega_{13})(x_2 - \omega_{12}x_1)]}{\sqrt{[(1 - \omega_{12}^2)(\nu + x_1^2) + (x_2 - \omega_{12}x_1)^2] [(1 - \omega_{12}^2)(1 - \omega_{13}^2) - (\omega_{23} - \omega_{12}\omega_{13})^2]}}; \nu + 2 \right) \\
& \times \psi(v_{2 \cdot 1}; \nu + 1) \sqrt{\frac{\nu + 1}{1 - \omega_{12}^2}} \frac{2(x_2x_1 + \omega_{12}\nu)(\nu + 2)x_1 - \nu(x_2 - \omega_{12}x_1)}{(\nu + x_1^2)^{3/2}} \\
& \times \frac{(\nu + 2)(x_2 - \omega_{12}x_1)\sqrt{\nu + 1}(x_2x_1 + \omega_{12}\nu)^2}{\sqrt{1 - \omega_{12}^2}(\nu + x_1^2)^{3/2} ((1 - \omega_{12}^2)(\nu + x_1^2) + (x_2 - \omega_{12}x_1)^2)} \\
& + \Psi \left(\frac{\sqrt{\nu + 2} [(x_2 - \omega_{12}x_1)(1 - \omega_{13}^2) - (\omega_{23} - \omega_{12}\omega_{13})(x_3 - \omega_{13}x_1)]}{\sqrt{[(1 - \omega_{13}^2)(\nu + x_1^2) + (x_3 - \omega_{13}x_1)^2] [(1 - \omega_{12}^2)(1 - \omega_{13}^2) - (\omega_{23} - \omega_{12}\omega_{13})^2]}}; \nu + 2 \right) \\
& \times \psi(v_{3 \cdot 1}; \nu + 1) \sqrt{\frac{\nu + 1}{1 - \omega_{13}^2}} \frac{2(x_3x_1 + \omega_{13}\nu)(\nu + 2)x_1 - \nu(x_3 - \omega_{13}x_1)}{(\nu + x_1^2)^{3/2}} \\
& \times \frac{(\nu + 2)(x_3 - \omega_{13}x_1)\sqrt{\nu + 1}(x_3x_1 + \omega_{13}\nu)^2}{\sqrt{1 - \omega_{13}^2}(\nu + x_1^2)^{3/2} ((1 - \omega_{13}^2)(\nu + x_1^2) + (x_3 - \omega_{13}x_1)^2)} \\
& + \psi \left(\frac{\sqrt{\nu + 2} [(x_3 - \omega_{13}x_1)(1 - \omega_{12}^2) - (\omega_{23} - \omega_{12}\omega_{13})(x_2 - \omega_{12}x_1)]}{\sqrt{[(1 - \omega_{12}^2)(\nu + x_1^2) + (x_2 - \omega_{12}x_1)^2] [(1 - \omega_{12}^2)(1 - \omega_{13}^2) - (\omega_{23} - \omega_{12}\omega_{13})^2]}}; \nu + 2 \right) \\
& \times \psi(v_{2 \cdot 1}; \nu + 1) \sqrt{\frac{(1 - \omega_{12}^2)(\nu + 2)}{(1 - \omega_{12}^2)(1 - \omega_{13}^2) - (\omega_{23} - \omega_{12}\omega_{13})^2}} \\
& \times \frac{\sqrt{\nu + 1}(x_2x_1 + \omega_{12}\nu)}{\sqrt{\nu + x_1^2}((1 - \omega_{12}^2)(\nu + x_1^2) + (x_2 - \omega_{12}x_1)^2)^{3/2}} \left[((1 - \omega_{12}^2)(\nu + x_1^2) + (x_2 - \omega_{12}x_1)^2) \right. \\
& \times \left(\omega_{12} \frac{\omega_{23} - \omega_{12}\omega_{13}}{1 - \omega_{12}^2} - \omega_{13} \right) - \left((x_3 - \omega_{13}x_1) - \frac{\omega_{23} - \omega_{12}\omega_{13}}{1 - \omega_{12}^2} (x_2 - \omega_{12}x_1) \right) (x_1 - \omega_{12}x_2) \left. \right] \\
& + \psi \left(\frac{\sqrt{\nu + 2} [(x_2 - \omega_{12}x_1)(1 - \omega_{13}^2) - (\omega_{23} - \omega_{12}\omega_{13})(x_3 - \omega_{13}x_1)]}{\sqrt{[(1 - \omega_{13}^2)(\nu + x_1^2) + (x_3 - \omega_{13}x_1)^2] [(1 - \omega_{12}^2)(1 - \omega_{13}^2) - (\omega_{23} - \omega_{12}\omega_{13})^2]}}; \nu + 2 \right) \\
& \times \psi(v_{3 \cdot 1}; \nu + 1) \sqrt{\frac{(1 - \omega_{13}^2)(\nu + 2)}{(1 - \omega_{12}^2)(1 - \omega_{13}^2) - (\omega_{23} - \omega_{12}\omega_{13})^2}} \\
& \times \frac{\sqrt{\nu + 1}(x_3x_1 + \omega_{13}\nu)}{\sqrt{\nu + x_1^2}((1 - \omega_{13}^2)(\nu + x_1^2) + (x_3 - \omega_{13}x_1)^2)^{3/2}} \left[((1 - \omega_{13}^2)(\nu + x_1^2) + (x_3 - \omega_{13}x_1)^2) \right. \\
& \times \left(\omega_{13} \frac{\omega_{23} - \omega_{12}\omega_{13}}{1 - \omega_{13}^2} - \omega_{12} \right) - \left((x_2 - \omega_{12}x_1) - \frac{\omega_{23} - \omega_{12}\omega_{13}}{1 - \omega_{13}^2} (x_3 - \omega_{13}x_1) \right) (x_1 - \omega_{13}x_3) \left. \right].
\end{aligned}$$

Combining the derivatives of the t cdf with equations (28)-(31) provides the full d -dimensional densities of the extremal- t process. Returning to the extremal skew- t case (i.e. when $\alpha \neq 0$ and $\tau \neq 0$), it is sufficient to consider the following changes. Firstly, rewrite

$$T_j = \frac{\Psi_d \left\{ \begin{pmatrix} u_j \\ \bar{\tau}_j \end{pmatrix}; \begin{pmatrix} \bar{\Omega}_j^\circ & -\delta_j \\ -\delta_j^\top & 1 \end{pmatrix}, \nu + 1 \right\}}{\Psi_1(\bar{\tau}_j; \nu + 1)}, \quad j \in I,$$

where $u_j = \left[\sqrt{\frac{\nu+1}{1-\omega_{i,j}^2}} \left\{ \left(\frac{x_i^\circ}{x_j^\circ} \right)^{1/\nu} - \omega_{i,j} \right\}, i \in I_j \right]^\top$, following Definition 1. It can then be shown that

$$V_{1 \dots d} = -(\nu x_1)^{-(d+1)} \psi_{d-1}(u_1; \bar{\Omega}_1^\circ, \alpha_1^\circ, \tau_1^\circ, \kappa_1^\circ, \nu + 1) \prod_{i=2}^d \sqrt{\frac{\nu+1}{1-\omega_{i,1}^2}} \left(\frac{x_i^\circ}{x_1^\circ} \right)^{\frac{1}{\nu}-1} \frac{m_i^+}{m_1^+}$$

following Theorem 1. Note that equations (28)–(31) are still valid in this case, through the redefinition of $d \leftarrow d + 1$ and $u_j \leftarrow (u_j, \bar{\tau}_j)^\top$. This in combination with the above derivatives of the t cdfs leads to the d -dimensional densities of the extremal-skew- t process.

References

Arellano-Valle, R. B. and A. Azzalini (2006). On the unification of families of skew-normal distributions. *Scandinavian Journal of Statistics*, 561–574.

Arellano-Valle, R. B. and M. G. Genton (2010). Multivariate extended skew- t distributions and related families. *Metron* 68(3), 201–234.

Azzalini, A. (1985). A class of distributions which includes the normal ones. *Scandinavian journal of statistics*, 171–178.

Azzalini, A. (2005). The skew-normal distribution and related multivariate families. *Scand. J. Statist.* 32(2), 159–200. With discussion by Marc G. Genton and a rejoinder by the author.

Azzalini, A. (2013). *The skew-normal and related families*, Volume 3. Cambridge University Press.

Bortot, P. (2010). Tail dependence in bivariate skew-normal and skew- t distributions.

Brown, B. M. and S. I. Resnick (1977). Extreme values of independent stochastic processes. *Journal of Applied Probability*, 732–739.

Chan, G. and A. T. Wood (1997). Algorithm as 312: An algorithm for simulating stationary gaussian random fields. *Journal of the Royal Statistical Society: Series C (Applied Statistics)* 46(1), 171–181.

Chang, S.-M. and M. G. Genton (2007). Extreme value distributions for the skew-symmetric family of distributions. *Communications in Statistics—Theory and Methods* 36(9), 1705–1717.

Coles, S. G. and J. A. Tawn (1991). Modelling extreme multivariate events. *Journal of the Royal Statistical Society. Series B (Methodological)* 53(2), pp. 377–392.

Coles, S. G. and J. A. Tawn (1994). Statistical methods for multivariate extremes: An application to structural design. *Journal of the Royal Statistical Society. Series C (Applied Statistics)* 43(1), pp. 1–48.

Davison, A. C. and M. M. Gholamrezaee (2012). Geostatistics of extremes. *Proceedings of the Royal Society of London Series A: Mathematical and Physical Sciences* 468, 581–608.

Davison, A. C., S. A. Padoan, and M. Ribatet (2012). Statistical Modeling of Spatial Extremes. *Statistical Science* 27, 161–186.

de Haan, L. (1984). A spectral representation for max-stable processes. *Ann. Probab.* 12(4), 1194–1204.

de Haan, L. and A. Ferreira (2006). *Extreme value theory*. Springer Series in Operations Research and Financial Engineering. Springer, New York. An introduction.

Dutt, J. E. (1973). A representation of multivariate normal probability integrals by integral transforms. *Biometrika* 60(3), 637–645.

Feller, W. (1968). An introduction to probability theory, vol. 1.

Genton, M. (2004). *Skew-elliptical distributions and their applications*. Chapman & Hall/CRC, Boca Raton, FL. A journey beyond normality, Edited by Marc G. Genton.

Huser, R. and A. C. Davison (2013). Composite likelihood estimation for the Brown-Resnick process. *Biometrika* 100(2), 511–518.

Huser, R. and M. Genton (2015). Non-stationary dependence structures for spatial extremes. *arXiv:1411.3174v1*.

Jamalizadeh, A., Y. Mehrali, and N. Balakrishnan (2009). Recurrence relations for bivariate t and extended skew-t distributions and an application to order statistics from bivariate t. *Computational Statistics & Data Analysis* 53(12), 4018–4027.

Joe, H. (1997). *Multivariate models and dependence concepts*, Volume 73 of *Monographs on Statistics and Applied Probability*. Chapman & Hall, London.

Kabluchko, Z., M. Schlather, and L. De Haan (2009). Stationary max-stable fields associated to negative definite functions. *The Annals of Probability*, 2042–2065.

Ledford, A. W. and J. A. Tawn (1996). Statistics for near independence in multivariate extreme values. *Biometrika* 83(1), 169–187.

Lindgren, G. (2012). *Stationary Stochastic Processes: Theory and Applications*. CRC Press.

Lysenko, N., P. Roy, and R. Waeber (2009). Multivariate extremes of generalized skew-normal distributions. *Statist. Probab. Lett.* 79(4), 525–533.

Minozzo, M. and L. Ferracuti (2012). On the existence of some skew-normal stationary processes. *Chilean Journal of Statistics* 3, 157–170.

Nikoloulopoulos, A. K., H. Joe, and H. Li (2009). Extreme value properties of multivariate t copulas. *Extremes* 12(2), 129–148.

Opitz, T. (2013). Extremal t processes: Elliptical domain of attraction and a spectral representation. *Journal of Multivariate Analysis* 122(0), 409 – 413.

Padoan, S. A. (2011). Multivariate extreme models based on underlying skew- and skew-normal distributions. *Journal of Multivariate Analysis* 102(5), 977 – 991.

Padoan, S. A., M. Ribatet, and S. A. Sisson (2010). Likelihood-Based Inference for Max-Stable Processes. *Journal of the American Statistical Association* 105(489), 263–277.

Schlather, M. (2002). Models for stationary max-stable random fields. *Extremes* 5(1), 33–44.

Smith, R. L. (1990). Max-stable processes and spatial extremes. University of Surrey 1990 technical report.

Thibaud, E. and T. Optiz (2015). Efficient inference and simulation for elliptical pareto processes. *Biometrika* to appear.

Varin, C., N. Reid, and D. Firth (2011). An overview of composite likelihood methods. *Statist. Sinica* 21(1), 5–42.

Wood, A. T. and G. Chan (1994). Simulation of stationary gaussian processes in $[0, 1]$ d. *Journal of computational and graphical statistics* 3(4), 409–432.

Zhang, H. and A. El-Shaarawi (2010). On spatial skew-gaussian processes and applications. *Environmetrics* 21(1), 33–47.

$\nu = 1$					
$n = 20$					
$\lambda \setminus \xi$	0.5	1	1.5	1.9	2
14	89/94/89	84/97/93	83/69/79	81/82/84	78/64/72
28	76/100/98	59/100/69	73/86/73	74/66/75	34/75/26
42	81/100/100	51/96/89	51/80/88	43/63/79	33/51/72
$n = 50$					
$\lambda \setminus \xi$	0.5	1	1.5	1.9	2
14	85/81/84	87/78/86	76/67/78	66/56/72	52/47/62
28	64/100/81	81/79/82	73/72/78	72/66/74	34/68/24
42	71/100/97	33/61/59	17/42/40	17/34/37	2/18/7
$n = 70$					
$\lambda \setminus \xi$	0.5	1	1.5	1.9	2
14	80/87/83	81/76/80	74/65/77	62/57/70	47/42/60
28	51/100/68	82/82/84	72/72/77	71/66/73	54/53/62
42	56/93/89	28/52/48	13/40/14	12/28/27	8/23/26

$\nu = 3$					
$n = 20$					
$\lambda \setminus \xi$	0.5	1	1.5	1.9	2
14	93/100/96	93/96/91	88/84/83	84/83/84	78/77/82
28	86/100/100	72/97/75	90/91/89	87/85/86	39/78/50
42	78/100/100	72/97/100	58/71/74	51/68/95	44/58/84

$n = 50$					
$\lambda \setminus \xi$	0.5	1	1.5	1.9	2
14	91/85/89	92/89/92	86/81/88	82/78/86	64/64/74
28	70/100/81	74/87/63	83/81/84	80/74/82	77/75/81
42	69/100/100	47/70/75	36/53/64	30/40/61	38/32/33

$n = 70$					
$\lambda \setminus \xi$	0.5	1	1.5	1.9	2
14	93/93/94	89/88/87	81/77/85	81/74/84	58/58/71
28	94/94/94	85/87/89	81/77/86	79/75/82	81/77/84
42	65/94/95	44/57/62	29/45/49	25/35/50	20/28/38

Table 2: Efficiency of maximum triplewise likelihood estimators relative to maximum pairwise likelihood estimators for the Extremal- t process, based on 300 replicate simulations. Simulated datasets of size $n = 20, 50, 70$ are generated at 20 random sites in $\mathbb{S} = [0, 100]^2$, given power exponential dependence function parameters $\vartheta = (\lambda, \xi)$. Relative efficiencies are $RE_\xi/RE_\lambda/RE_{(\lambda, \xi)}$ ($\times 100$) where $RE_\xi = \widehat{\text{var}}(\hat{\xi}_3)/\widehat{\text{var}}(\hat{\xi}_2)$, $RE_\lambda = \widehat{\text{var}}(\hat{\lambda}_3)/\widehat{\text{var}}(\hat{\lambda}_2)$ and $RE_{(\lambda, \xi)} = \widehat{\text{cov}}(\hat{\lambda}_3, \hat{\xi}_3)/\widehat{\text{cov}}(\hat{\lambda}_2, \hat{\xi}_2)$, where $(\hat{\lambda}_p, \hat{\xi}_p)$ are the p -wise maximum composite likelihood estimates ($p = 2, 3$), and $\widehat{\text{var}}$ and $\widehat{\text{cov}}$ denote sample variance and covariance over replicates.